ARL-TR-8561 • Oct 2018

US Army Research Laboratory

The Rigid-Body Dynamics of a Spinning Axisymmetric Body Subject to an Impulsive Mass Ejection

by Steven B Segletes

NOTICES

Disclaimers

ARL-TR-8561 • OCT 2018

US Army Research Laboratory

The Rigid-Body Dynamics of a Spinning Axisymmetric Body Subject to an Impulsive Mass Ejection

by Steven B Segletes
Weapons and Materials Research Directorate, ARL

Approved for public release; distribution is unlimited.

REPORT DOCUMENTATION PAGE	*Form Approved* *OMB No. 0704-0188*

1. REPORT DATE *(DD-MM-YYYY)*	October 2018
2. REPORT TYPE	Technical Report
3. DATES COVERED (From - To)	May 2018–Aug 2018
4. TITLE AND SUBTITLE	The Rigid-Body Dynamics of a Spinning Axisymmetric Body Subject to an Impulsive Mass Ejection
5a. CONTRACT NUMBER	
5b. GRANT NUMBER	
5c. PROGRAM ELEMENT NUMBER	
6. AUTHOR(S)	Steven B Segletes
5d. PROJECT NUMBER	AH80
5e. TASK NUMBER	
5f. WORK UNIT NUMBER	
7. PERFORMING ORGANIZATION NAME(S) AND ADDRESS(ES)	US Army Research Laboratory ATTN: RDRL-WMP-C Aberdeen Proving Ground, MD 21005-5066
8. PERFORMING ORGANIZATION REPORT NUMBER	ARL-TR-8561
9. SPONSORING/MONITORING AGENCY NAME(S) AND ADDRESS(ES)	
10. SPONSOR/MONITOR'S ACRONYM(S)	
11. SPONSOR/MONITOR'S REPORT NUMBER(S)	
12. DISTRIBUTION/AVAILABILITY STATEMENT	Approved for public release; distribution is unlimited.
13. SUPPLEMENTARY NOTES	author's email: <steven.b.segletes.civ@mail.mil>.

14. ABSTRACT

The rotational motion of bodies is a well-understood branch of dynamics. In this report, we apply those methods to study the problem of a spinning axisymmetric body that, in an instant, impulsively ejects a portion of its mass radially from the residual body. Not only is the residual body no longer axisymmetric, but the process of ejecting mass induces changes to the linear and rotational momentum of the residual body, as well as to its inertial properties. The ejection also produces precessive motion in the residual body. This report solves for the net state of the body in the immediate aftermath of the mass ejection. It then considers both an axisymmetric approximation to the residual motion, if the mass ejection is small, or, for the general case, solves the rotational momentum and energy equations in the body frame of reference, using a novel variation on a geometrical approach. The results of these analyses allow one to determine the range of precessive motion of the residual body.

15. SUBJECT TERMS

precession, non-axisymmetry, moment of inertia, spinning

16. SECURITY CLASSIFICATION OF: a. REPORT	b. ABSTRACT	c. THIS PAGE	17. LIMITATION OF ABSTRACT	18. NUMBER OF PAGES	19a. NAME OF RESPONSIBLE PERSON / 19b. TELEPHONE NUMBER (Include area code)
Unclassified	Unclassified	Unclassified	UU	62	Steven B Segletes 410-278-6010

Standard Form 298 (Rev. 8/98)
Prescribed by ANSI Std. Z39.18

Contents

List of Figures

List of Tables

Acknowledgments

The author is extremely indebted to his colleague Adam Sokolow, not only for reviewing this report, but for the productive technical discussions concerning the implications of non-axisymmetry upon the equations governing torque-free rotation. The author is, once again, extremely grateful to his editor, Carol Johnson, for her efforts in improving the content and presentation of this report.

1. Introduction

The rotational motion of bodies is a well-understood branch of dynamics. In this report, we apply those methods to study the problem of a freely spinning axisymmetric body that, in an instant, impulsively ejects a portion of its mass radially from the residual body. Not only is the residual body no longer axisymmetric, but the process of ejecting mass induces changes to the linear and rotational momentum of the residual body, brought about by the equal and opposite forces between the ejected mass and the residual body.

As a result of all these influences, the ejection produces precessive motion in the residual body. We wish to derive the motion of the residual body (or at least its limits of motion), to gauge resultant changes to its principal axes, precessive angle, and center of gravity (CG). There exist textbook treatments that account for impulsive loads to spinning bodies.* However, in Beer and Johnston,[1] for example, there is no accounting for any mass ejection from the spinning body.

2. The Problem

Consider an axisymmetric body of mass M to be rotating with angular velocity ω_0 about its axis of symmetry, the z-axis, such that $\boldsymbol{\omega}_0 = (0,\, 0,\, \omega_0)$. The situation, before and after the mass ejection, is represented in the schematic Fig. 1. Because the system is initially axisymmetric, the figure takes the liberty, with no loss of generality, to define the laboratory coordinate system so that the mass m, at the moment of ejection, resides in the y-z plane.

The principal moment of inertia about the z-axis (the spin axis) is given as $J_s = J_{zz}$, whereas the moment of inertia about the transverse principal axes is $J_t = J_{xx} = J_{yy}$, such that

$$\mathbf{J}_G = \begin{bmatrix} J_t & 0 & 0 \\ 0 & J_t & 0 \\ 0 & 0 & J_s \end{bmatrix} \tag{1}$$

defines the principal moment of inertia tensor of the body (which is, by definition, taken about the CG, denoted here as G). For slender (prolate) bodies of rotation, of interest to our analysis, it will be the case that $J_t > J_s$.

*The sample problem 18.6, on p. 864 of Beer and Johnston[1] provides some measure of background for what is being done here.

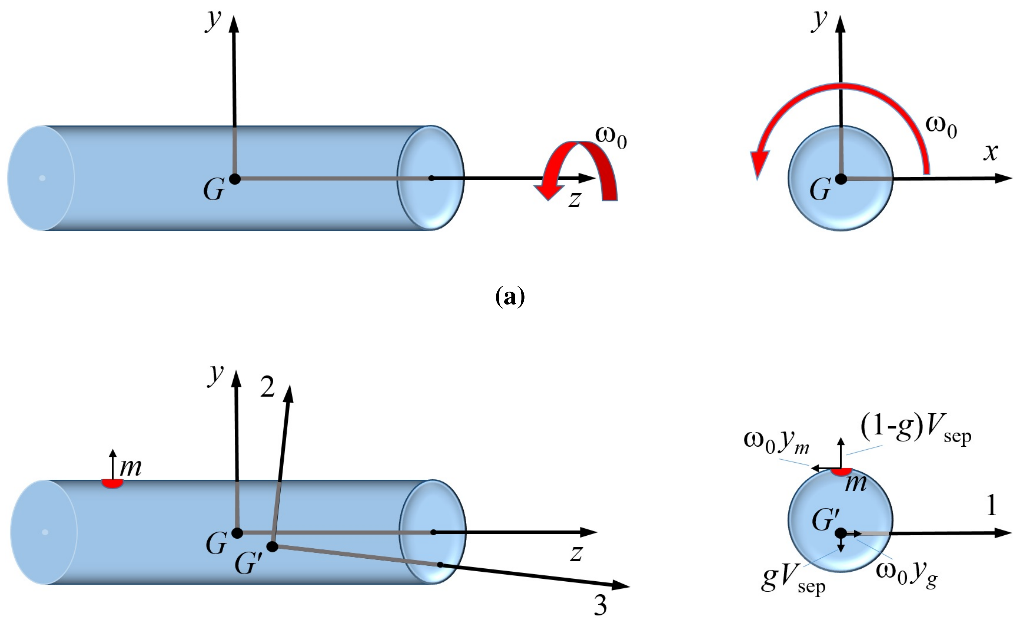

(a)

(b)

Fig. 1 Schematic of the (a) original and (b) residual bodies following the ejection of mass

Figure 1b shows, at a moment in time, a small* portion of the body mass, m, vectorially located (relative to G) at $\mathbf{r}_m = (x_m,\, y_m,\, z_m)$, impulsively ejected† from the surface of the original body. The relative separation velocity is normal to the body surface and of magnitude V_{sep}, where the surface normal may be specified as $\mathbf{n}_m = (n_x,\, n_y,\, n_z)$. Note that the ejected mass m also has a velocity component tangential to the axisymmetric surface, matching that on the residual body, owing to the original body's spin and given vectorially as $\boldsymbol{\omega}_0 \times \mathbf{r}_m$. This mass ejection has a number of noteworthy effects on the system:

1. The CG of the residual body is altered (from G) to G'.
2. The moment of inertia of the residual body is altered, including the orientation of its principal axes, from the x-y-z coordinates to a rotated 1-2-3 system.
3. There is an impulsive force, equal and opposite, between the residual body and ejected mass, acting normal to the body surface.
4. The residual body is no longer axisymmetric, under the influence of point

*By "small", several things are implied: the ejected mass is much less than the original body mass, and the ejected mass can be considered to originate from a point in space.

†Note that, in the mathematical treatment that follows throughout this report, the ejected mass m and its normal separation velocity V_{sep}, may be taken as negative, with no loss of generality, to represent the situation where mass is impulsively *added to* the original body.

mass loss. However, if the ejected mass m is suitably small, axisymmetric approximation of the residual body may still be possible.

Because of the impulsive nature of the event, we are ignoring the effects of gravity and, more generally, all aero effects that can couple the gas upon the body (as these effects occur over longer periods of time) and focus solely upon the effects of mass loss and impulsive load upon the gyroscopic response of the body.

We use the term "small" to denote the ejected mass m so that we may consider it to be concentrated at the point $\mathbf{r}_m$ relative to the body's pre-ejection CG, which is given by G. We define the coordinate system relative to G so that the coordinates of G are by definition $(0, 0, 0)$, with the z-axis aligned with the original body's axis of symmetry.

3. The Governing Equations

Any dynamics analysis of rigid bodies must be concerned with the following elements: moments of inertia, linear and angular momenta, along with the coordinate transformations to and from the body's principal reference frame. Next, these aspects are considered for the problem at hand: that of a spinning body, which impulsively ejects a portion of its mass. The analysis first considers the general case, and then, where appropriate, simplifies the result for the axisymmetric initial conditions that prevail for the problem under consideration.

3.1 Linear Momentum

Considering the residual body plus the ejected mass as a closed system, momentum is conserved before and after the ejection. Since the original body is in a state of pure rotation (in our inertial coordinate system attached to G), there is zero net linear momentum in the system. This must be preserved following the ejection.

However, in the process of ejecting mass m, the CG of the residual body relocates from G to G' by an amount $\mathbf{r}_{G'} = (x_{G'},\, y_{G'},\, z_{G'})$. Furthermore, the amount of CG translation, $\mathbf{r}_{G'}$, may be expressed directly in terms of the ejected mass m and its location, by the following proportional relationship*:

$$(M-m)\,\mathbf{r}_{G'} = -m\,\mathbf{r}_m \quad . \tag{2}$$

If we let g denote the ratio

$$g = \frac{m}{M} \quad , \tag{3}$$

then, from Eq. 2,

$$(1-g)\,\mathbf{r}_{G'} = -g\,\mathbf{r}_m \quad , \tag{4}$$

so that g is seen to not only represent a mass ratio, but also a length ratio (applying uniformly to the x, y, and z-coordinates of $\mathbf{r}_m$ and $\mathbf{r}_{G'}$).

In the defined coordinate system, where the ejected mass m falls in the y-z plane at the moment of ejection, it immediately follows that $x_m = n_x = x_{G'} = 0$. Furthermore, all velocities in the x-direction are due to the initial spin of the body and any net velocity in the y-z plane results from the impulsive ejection of mass m.

First, let us conserve momentum in the x direction. Denoting the x-components of velocity of m and G' as V_{mx} and $V_{G'x}$, respectively,

$$\begin{aligned} V_{mx} &= \boldsymbol{\omega}_0 \times \mathbf{r}_m = -\omega_0\, y_m \\ V_{G'x} &= \boldsymbol{\omega}_0 \times \mathbf{r}_{G'} = -\omega_0\, y_{G'} \end{aligned} \quad .$$

Momentum conservation in the x-direction, namely,

$$mV_{mx} + (M-m)V_{G'x} = 0 \quad ,$$

leads, by way of Eq. 4, to the tautology

$$\frac{(m/M)}{1-(m/M)} = -\frac{V_{G'x}}{V_{mx}} = -\frac{y_{G'}}{y_m} = \frac{g}{1-g} \quad .$$

Thus, satisfying x-momentum conservation is redundant to properly calculating the revised-body CG in terms of the ejected mass location (Eq. 2).

To satisfy momentum conservation in the y-z plane, we note that the equal and

*In each coordinate direction, the areal moments (about G) of the to-be-removed mass (*e.g.*, $m\,\mathbf{r}_m$) and the to-be-residual mass (*e.g.*, $(M-m)\,\mathbf{r}_{G'}$) must sum to zero. Once m has been ejected, the residual body's CG (*i.e.*, G') is, by definition, located at $\mathbf{r}_{G'}$.

opposite impulse applied to the ejected mass and the residual body are directed along the $\mathbf{n}$ vector (the surface normal at the ejection point), so that the scalar balance

$$mV_{m(yz)} + (M - m)V_{G'(yz)} = 0$$

must be satisfied, from which emerges the deduction that

$$\frac{V_{G'(yz)}}{V_{m(yz)}} = -\frac{g}{1-g} \quad .$$

We use the subscript (yz) to denote a vectorial component projected as a scalar magnitude in the y-z plane (the scalar projection is parallel to and, thus, independent of $\mathbf{n}$). Yet, we know from the initial condition (relative separation velocity) that

$$V_{m(yz)} - V_{G'(yz)} = V_{\text{sep}} \quad ,$$

so that, along the direction of $\mathbf{n}$,

$$\begin{aligned} V_{m(yz)} &= (1-g)V_{\text{sep}} \\ V_{G'(yz)} &= -gV_{\text{sep}} \end{aligned} \quad .$$

The velocity ratio in the y-z plane matches those in the x-direction, so that we may generalize vectorially as

$$(1-g)\,\mathbf{V}_{G'} = -g\,\mathbf{V}_m \quad .$$

Expressing explicitly in the x-y-z coordinate frame, the linear velocities of the ejected mass and the residual body are, respectively,

$$\begin{aligned} \mathbf{V}_m &= (1-g)\left(-\omega_0(y_m - y_{G'}),\ n_y V_{\text{sep}},\ n_z V_{\text{sep}}\right) \\ \mathbf{V}_{G'} &= \qquad -g\left(-\omega_0(y_m - y_{G'}),\ n_y V_{\text{sep}},\ n_z V_{\text{sep}}\right) \end{aligned} \quad . \tag{5}$$

3.2 Moment of Inertia

The contribution that the ejected mass m made to the original body's moment of inertia[*] (relative to the original CG, given by G) is

$$\mathbf{J}_m = m \cdot \begin{bmatrix} (y_m^2 + z_m^2) & -x_m y_m & -x_m z_m \\ -x_m y_m & (x_m^2 + z_m^2) & -y_m z_m \\ -x_m z_m & -y_m z_m & (x_m^2 + y_m^2) \end{bmatrix} \quad . \tag{6}$$

Therefore, the moment of inertia of the residual body, at the moment immediately following the ejection of mass m, taken relative to G is

$$\mathbf{J}'_G = \mathbf{J}_G - \mathbf{J}_m \quad .$$

However, as noted already, the ejection of mass m relocates the CG of the residual body from G to G' by an amount $\mathbf{r}_{G'} = (x_{G'},\, y_{G'},\, z_{G'})$. The moment of inertia of the residual body, accounting for the coordinate translation from G to G', may be obtained with a textbook application of the parallel axis theorem, such that

$$\begin{aligned} \mathbf{J}'_{G'} &= \mathbf{J}'_G - \Delta\mathbf{J}_G \\ &= \mathbf{J}_G - (\mathbf{J}_m + \Delta\mathbf{J}_G) \end{aligned} \quad . \tag{7}$$

where

$$\Delta\mathbf{J}_G = (M - m) \cdot \begin{bmatrix} (y_{G'}^2 + z_{G'}^2) & 0 & 0 \\ 0 & (x_{G'}^2 + z_{G'}^2) & 0 \\ 0 & 0 & (x_{G'}^2 + y_{G'}^2) \end{bmatrix} \quad .$$

From Eq. 2, the amount of CG translation, $\mathbf{r}_{G'}$, may be expressed directly in terms of the ejected mass m and its location $\mathbf{r}_m$, so that ΔJ_G may be re-expressed in terms of the $\mathbf{r}_m$ components as

$$\Delta\mathbf{J}_G = \frac{m}{M - m}\, m \cdot \begin{bmatrix} (y_m^2 + z_m^2) & 0 & 0 \\ 0 & (x_m^2 + z_m^2) & 0 \\ 0 & 0 & (x_m^2 + y_m^2) \end{bmatrix} \quad .$$

[*]Note that the simple form of Eq. 6 derives from our approximating the mass ejection as originating from a point. That approximation can be removed simply by replacing Eq. 6 with a form that accounts for the distributed nature of the actual mass ejection.

We note that the diagonal terms of $\Delta\mathbf{J}_G$ are related to those of $\mathbf{J}_m$ via

$$\Delta\mathbf{J}_{G(ii)} = \frac{m}{M-m}\mathbf{J}_{m(ii)} \qquad \text{(no sum)} \quad . \tag{8}$$

If we let f denote the complement of g (Eq. 3), such that

$$f = 1 - g = \frac{M-m}{M} \quad , \tag{9}$$

then the sum $\mathbf{J}_m + \Delta\mathbf{J}_G$ may be expressed as

$$\mathbf{J}_m + \Delta\mathbf{J}_G = m \cdot \begin{bmatrix} (y_m^2 + z_m^2)/f & -x_m y_m & -x_m z_m \\ -x_m y_m & (x_m^2 + z_m^2)/f & -y_m z_m \\ -x_m z_m & -y_m z_m & (x_m^2 + y_m^2)/f \end{bmatrix} \quad . \tag{10}$$

Note that, while $\mathbf{r}_m$ is the distance to the ejected mass m relative to the *original body* CG, $\mathbf{r}_m - \mathbf{r}_{G'}$ is the distance to the ejected mass, relative to the *residual* (post-ejection) CG.

Equation 10 allows the description of $\mathbf{J}'_{G'}$, given by Eq. 7, to be given as

$$\mathbf{J}'_{G'} = m \cdot \begin{bmatrix} \dfrac{J_t}{m} - \dfrac{y_m^2 + z_m^2}{f} & x_m y_m & x_m z_m \\ x_m y_m & \dfrac{J_t}{m} - \dfrac{x_m^2 + z_m^2}{f} & y_m z_m \\ x_m z_m & y_m z_m & \dfrac{J_s}{m} - \dfrac{x_m^2 + y_m^2}{f} \end{bmatrix} \quad . \tag{11}$$

It is worthy to note that the G' coordinate system represents a *translation* from system G. Because of the loss of mass m, the revised moment of inertia matrix, $\mathbf{J}'_{G'}$, is no longer diagonal (in the general case) and must be rotated to determine the new principal axes of the body. While the analysis to this point makes use of an assumption that the mass ejection can be treated as an event originating from a point, there is nothing that prevents $\mathbf{J}'_{G'}$ from being more assiduously calculated through less assumptive means, in lieu of Eq. 11.

3.2.1 Axisymmetric Simplification to the Moment of Inertia

The axisymmetric simplification to the moment of inertia, for the original body, is already contained in Eq. 1, wherein the axis of symmetry is aligned with the z-axis and $J_{xx} = J_{yy} = J_t$. The ejection of mass m, however, is not axisymmetric and so Eq. 11 cannot be made axisymmetric. Nonetheless, simplification will arise in that, because the original body was axisymmetric, a laboratory x-y-z coordinate system may always be chosen to insure that the mass ejection occurs in, for example, the y-z plane without requiring alteration of Eq. 1. When this is done, $x_m = x_{G'} = 0$ can be assured. Further, because the original body was axisymmetric, it is also the case that the surface-normal component $n_x = 0$.

3.3 Transforming to and from the Principal Frame

As of Section 3.2, coordinate transformations were limited to translations from the original body's CG, given by G, to the CG of the residual body, given by G', following the ejection of mass m. Some calculations are, however, simpler when performed in the reference frame that is aligned with the principal axes of the body.

Let us examine the textbook method for rotationally transforming tensors and vectors to and from the principal coordinate system and apply the method to the problem of moment of inertia. For convenience, denote the elements of $\mathbf{J}'_{G'}$ (Eq. 11) as

$$\mathbf{J}'_{G'} = \begin{bmatrix} J'_{xx} & J'_{xy} & J'_{xz} \\ J'_{yx} & J'_{yy} & J'_{yz} \\ J'_{zx} & J'_{zy} & J'_{zz} \end{bmatrix} \quad .$$

To obtain the principal moments for this nondiagonal $\mathbf{J}'_{G'}$, we must obtain the eigenvalues (principal inertias) and eigenvectors (principal directions) of $\mathbf{J}'_{G'}$. The three eigenvalues are solved from $\det(\mathbf{J}'_{G'} - \lambda \mathbf{I}) = 0$, which in this case produces a cubic equation in λ:

$$\begin{vmatrix} J'_{xx} - \lambda & J'_{xy} & J'_{xz} \\ J'_{yx} & J'_{yy} - \lambda & J'_{yz} \\ J'_{zx} & J'_{zy} & J'_{zz} - \lambda \end{vmatrix} = 0 \quad , \tag{12}$$

which yields the three eigenvalue roots.

Once the three eigenvalues λ_i are obtained, the principal axes of inertia for the residual body correspond to the eigenvectors of $\mathbf{J}'_{G'}$. These eigenvectors $\mathbf{T}_i$ are obtained by solving, in turn, for each λ_i, the system

$$(\mathbf{J}'_{G'} - \lambda_i \mathbf{I})\mathbf{T}_i = \mathbf{0} \quad . \tag{13}$$

The eigenvectors $\mathbf{T}_i$ are expressed in the original x-y-z coordinate system and denote the orthonormal axial directions associated with the principal moments, λ_i.

Before the ejection of mass m, the principal axes of the body were aligned with the chosen x-y-z coordinate system in which the calculations have been performed. However, after the ejection, the principal axes of the body have changed. We know these revised principal axes to be the eigenvectors given by $\mathbf{T}_1$, $\mathbf{T}_2$, and $\mathbf{T}_3$. We, therefore, require the means to transform vectorial (and tensorial) quantities back and forth between the laboratory x-y-z coordinate system and the 1-2-3 coordinate system associated with the principal directions of the residual body.

A 3×3 transformation matrix, $\mathbb{T}$, may be constructed, such that each eigenvector $\mathbf{T}_i$ is successively placed as a column of $\mathbb{T}$. Namely,

$$\mathbb{T} = \Big[(\mathbf{T}_1) \quad (\mathbf{T}_2) \quad (\mathbf{T}_3)\Big] = \begin{bmatrix} T_{1x} & T_{2x} & T_{3x} \\ T_{1y} & T_{2y} & T_{3y} \\ T_{1z} & T_{2z} & T_{3z} \end{bmatrix} \quad . \tag{14}$$

The eigenvalues λ_i represent the principal moments of inertia of the residual body, such that

$$\hat{\mathbf{J}} = \begin{bmatrix} \lambda_1 & 0 & 0 \\ 0 & \lambda_2 & 0 \\ 0 & 0 & \lambda_3 \end{bmatrix} \quad .$$

It can be deduced that Eq. 13, $(\mathbf{J}'_{G'} - \lambda_i \mathbf{I})\mathbf{T}_i = \mathbf{0}$, is mathematically equivalent to the tensor rotational transformation relation, where the hat denotes the principal system:

$$\mathbb{T}^{\mathrm{T}} \mathbf{J}'_{G'} \mathbb{T} = \hat{\mathbf{J}} \quad .$$

The matrix $\mathbb{T}$ may also be used to transform vectorial quantities between the x-y-z coordinate system and the principal 1-2-3 coordinate system. Graphically, one may use direction cosines to successively project a vector $\mathbf{V}$ onto the principal axes $\mathbf{T}_i$, by way of

$$\begin{aligned}\hat{V}_1 &= \mathbf{T}_1 \cdot \mathbf{V}\\ \hat{V}_2 &= \mathbf{T}_2 \cdot \mathbf{V} \quad .\\ \hat{V}_3 &= \mathbf{T}_3 \cdot \mathbf{V}\end{aligned}$$

This, however, is equivalent to

$$\hat{\mathbf{V}} = \mathbb{T}^{\mathrm{T}}\mathbf{V} \quad . \tag{15}$$

Equation 15 transforms the vector $\mathbf{V}$, given in the x-y-z coordinate system, into a vector $\hat{\mathbf{V}}$ expressed in the principal coordinate system of the body. Because $\mathbf{T}_i$ compose an orthonormal set,* $\mathbb{T}$ is orthogonal and the inverse transformation may be accomplished with the transpose of $\mathbb{T}$, leading to

$$\mathbf{V} = \mathbb{T}\hat{\mathbf{V}} \quad . \tag{16}$$

Note that, in this report, all hatted quantities ($\hat{}$) are those expressed in the principal 1-2-3 coordinate reference frame.

3.3.1 Axisymmetric Simplification to the Coordinate Transformation

For our initially axisymmetric body, the problem of solving the cubic equation associated with Eq. 12 can be made a bit simpler. To do so, we choose our initial x and y (transverse) axes, such that the mass ejection always occurs in the y-z plane (therefore, y_m denotes the radial coordinate of the mass ejection relative to the original body's axis of symmetry, which traverses G). In this case, with $x_m = x_{G'} = 0$, it follows from Eq. 11 that $J'_{xy} = J'_{yx} = J'_{xz} = J'_{zx} = 0$, so that $\det(\mathbf{J}'_{G'} - \lambda\mathbf{I}) = 0$ simplifies to

$$(J'_{xx} - \lambda)\Big(\lambda^2 - (J'_{yy} + J'_{zz})\lambda + (J'_{yy}J'_{zz} - J'_{yz}J'_{zy})\Big) = 0 \quad .$$

*The eigenvectors $\mathbf{T}_i$ that describe the principal reference frame, given in Eq. 13 and later in Eq. 19, are expressed in the laboratory x-y-z frame of reference. Expressed in the principal 1-2-3 frame, they are simply (*i.e.*, by definition) $\hat{\mathbf{T}}_1 = (1, 0, 0)$, $\hat{\mathbf{T}}_2 = (0, 1, 0)$, and $\hat{\mathbf{T}}_3 = (0, 0, 1)$.

The solution for the eigenvalues now requires only the quadratic formula:

$$
\begin{aligned}
\lambda_1 &= J'_{xx} \\
\lambda_2 &= \frac{(J'_{yy} + J'_{zz}) \pm \sqrt{(J'_{yy} + J'_{zz})^2 - 4(J'_{yy}J'_{zz} - J'_{yz}J'_{zy})}}{2} \\
\lambda_3 &= \frac{(J'_{yy} + J'_{zz}) \mp \sqrt{(J'_{yy} + J'_{zz})^2 - 4(J'_{yy}J'_{zz} - J'_{yz}J'_{zy})}}{2}
\end{aligned}
\quad . \tag{17}
$$

These eigenvalues can be simplified* and expressed as

$$
\begin{aligned}
\lambda_1 &= J'_{xx} \\
\lambda_2 &= J'_{yy} + (Q - P) \\
\lambda_3 &= J'_{zz} - (Q - P)
\end{aligned}
\quad , \tag{18}
$$

where

$$
\begin{aligned}
P &= \frac{J'_{yy} - J'_{zz}}{2} \\
Q &= \operatorname{sgn}(P)\sqrt{P^2 + J'^2_{yz}}
\end{aligned}
$$

and the $\operatorname{sgn}(P)$ term dictates whether plus or minus was applied to the radical in Eq. 17. With only squared terms under the radical of Q, we may deduce several important points:

- All three eigenvalues of Eq. 17 are real.
- $Q = P$ if and only if $J'_{yz} = 0$.
- $|Q| > |P|$ for all nonzero values of J'_{yz}.
- From the definition of Q, we can express J'_{yz} as $\pm\sqrt{Q^2 - P^2}$.

*Exploiting the symmetry of $\mathbf{J}'_{G'}$, the λ_i described by Eq. 17 handily simplify to (as an intermediate step)

$$
\begin{aligned}
\lambda_1 &= J'_{xx} \\
\lambda_2 &= \frac{(J'_{yy} + J'_{zz}) \pm \sqrt{(J'_{yy} - J'_{zz})^2 + 4J'^2_{yz}}}{2} \\
\lambda_3 &= \frac{(J'_{yy} + J'_{zz}) \mp \sqrt{(J'_{yy} - J'_{zz})^2 + 4J'^2_{yz}}}{2}
\end{aligned}
\quad .
$$

- For prolate (slender) bodies of interest to us, under the constraint that $m \ll M$, it will be the case that $P > 0$ (based on the inference that $J'_{yy} > J'_{zz}$).

- From Eq. 11, with $x_m = 0$, we deduce that $J'_{yy} \geq J'_{xx}$ (as long as $m > 0$). For the prolate-body case under consideration, $Q - P \geq 0$. Thus, we may further deduce from Eq. 18 that $\lambda_2 \geq \lambda_1$. Therefore, the 1-axis is the intermediate inertial axis, so that $\lambda_2 \geq \lambda_1 > \lambda_3$. This ordering will have implications for non-axisymmetric rotational stability.

The eigenvectors $\mathbf{T}_i$ associated with λ_i, obtained from solving Eq. 13, are, respectively,

$$\begin{aligned}
\mathbf{T}_1 &= \left(1, \quad 0, \quad 0\right) \\
\mathbf{T}_2 &= \left(0, \quad \sqrt{\frac{Q+P}{2Q}}, \quad \operatorname{sgn}(J'_{yz})\sqrt{\frac{Q-P}{2Q}}\right) \\
\mathbf{T}_3 &= \left(0, \quad -\operatorname{sgn}(J'_{yz})\sqrt{\frac{Q-P}{2Q}}, \quad \sqrt{\frac{Q+P}{2Q}}\right)
\end{aligned} \quad , \tag{19}$$

as derived in the footnote.* The eigenvectors given by Eq. 19 may be composed

---

*Consider the second eigenvector $\mathbf{T}_2 = (v_1, v_2, v_3)$, associated with λ_2. The second equation of the system given by Eq. 13 tells us that $v_2/v_3 = [J'_{yz}/(Q-P)]$, leading to

$$\frac{v_2}{v_3} = \operatorname{sgn}(J'_{yz})\sqrt{\frac{Q^2-P^2}{(Q-P)^2}} = \operatorname{sgn}(J'_{yz})\sqrt{\frac{Q+P}{Q-P}} \ .$$

A comparable analysis can be performed for the third equation defining the third eigenvector $\mathbf{T}_3 = (w_1, w_2, w_3)$, associated with λ_3. In this case, one obtains $w_2/w_3 = -(Q-P)/J'_{yz}$, leading to, eventually,

$$\frac{w_2}{w_3} = -\operatorname{sgn}(J'_{yz})\sqrt{\frac{Q-P}{Q+P}} \ .$$

The expression of Eq. 19 is merely the normalized version of these concepts, where the $\pm$ signs have been chosen to keep $\mathbf{T}_2 \cdot (0,1,0) > 0$ and $\mathbf{T}_3 \cdot (0,0,1) > 0$.

Though not given here, it can be shown that the third equation for the λ_2 system (given by $J'_{yz}v_2 + (J'_{zz} - J'_{yy} + P - Q)v_3 = 0$) is redundant to the second equation ($(P-Q)v_2 + J'_{yz}v_3 = 0$) of the system. Likewise, the second equation of the λ_3 system ($(J'_{yy} - J'_{zz} + Q - P)w_2 + J'_{yz}w_3 = 0$) is redundant to the third equation of the system ($J'_{yz}w_2 + (Q-P)w_3 = 0$). These redundancies are a necessary requirement for eigenvectors.

into $\mathbb{T}$ (Eq. 14) as

$$\mathbb{T} = \begin{bmatrix} 1 & 0 & 0 \\ 0 & \sqrt{\dfrac{Q+P}{2Q}} & -\operatorname{sgn}(J'_{yz})\sqrt{\dfrac{Q-P}{2Q}} \\ 0 & \operatorname{sgn}(J'_{yz})\sqrt{\dfrac{Q-P}{2Q}} & \sqrt{\dfrac{Q+P}{2Q}} \end{bmatrix} \quad . \tag{20}$$

Based on the components of $\mathbf{T}_3 = (T_{3x},\, T_{3y},\, T_{3z})$ in Eq. 19, one may deduce that the principal axis, previously aligned with the original body's axis of symmetry, has rotated by an angle δ in the y-z plane:

$$\tan\delta = \frac{T_{3y}}{T_{3z}} = -\operatorname{sgn}(J'_{yz})\sqrt{\frac{Q-P}{Q+P}} \quad . \tag{21}$$

3.4 Angular Momentum

We consider the residual body *plus* the ejected mass as two elements of a closed system. Thus, no external force acts upon the system—the total angular momentum of the system, before and after mass ejection, are, therefore, identical. Beforehand, the CG is G, and the angular momentum about G is

$$\mathbf{H}_G = (0,\, 0,\, J_s\omega_0) \quad .$$

The amount of angular momentum afterward (with respect to G) remains unchanged. However, some angular momentum is locked up in the ejected mass m, which was located as $\mathbf{r}_m$. With respect to G, the amount of angular momentum locked up in the ejected mass m is

$$\mathbf{H}_m = m\,\mathbf{r}_m \times (\underbrace{\boldsymbol{\omega}_0 \times \mathbf{r}_m}_{\text{tangential}} + \underbrace{V_{\text{sep}}\,\mathbf{n}_m}_{\text{normal}}) \quad , \tag{22}$$

accounting for both the tangential and the normal velocity components of the ejected mass. The tangential velocity component, $\boldsymbol{\omega}_0 \times \mathbf{r}_m$, is preexisting, arising as a consequence of the original body spin, whereas the normal component, $V_{\text{sep}}\,\mathbf{n}_m$ (relative to G), is brought about by the normal interaction between the ejected mass and the residual body, during impulsive separation. Therefore, the post-ejection angular momentum of the residual body, relative to G, is

$$\mathbf{H}'_G = \mathbf{H}_G - \mathbf{H}_m \quad .$$

In the process of ejecting the mass m, the CG of the residual body moved from G to G', a translation of $(x_{G'},\ y_{G'},\ z_{G'})$. The angular momentum of the residual body, about G', is therefore given as

$$\begin{aligned} \mathbf{H}'_{G'} &= \mathbf{H}'_G - \Delta\mathbf{H}_G \\ & \mathbf{H}_G - (\mathbf{H}_m + \Delta\mathbf{H}_G) \end{aligned} \quad , \tag{23}$$

where $\Delta\mathbf{H}_G$ is made to account for both the difference in angular momentum of the residual body of mass $M - m$ taken relative to G' rather than G, as well as the difference in angular momentum of the ejected mass m taken relative to G' *vs.* G:

$$\Delta\mathbf{H}_G = \underbrace{(M - m)\,\mathbf{r}_{G'} \times \mathbf{V}_{G'/G}}_{\text{residual body}} + \underbrace{m\,\mathbf{r}_{G'} \times (V_{\text{sep}}\,\mathbf{n}_m)}_{\text{ejected mass}} \tag{24}$$

and $\mathbf{V}_{G'/G}$ is the velocity at G' relative to G.

3.4.1 Axisymmetric Simplification to the Angular Momentum

For our axisymmetric body, under the simplifying constraint of mass ejection in the y-z plane (see Fig. 1), we have $x_m = 0$ and $n_x = 0$, leading to

$$\begin{aligned} \boldsymbol{\omega}_0 \times \mathbf{r}_m &= (-\omega_0 y_m, 0, 0) \\ \mathbf{V}_{G'/G} &= (-\omega_0 y_{G'}, 0, 0) \end{aligned} \quad ,$$

so that, from Eq. 22,

$$\mathbf{H}_m = m\omega_0 y_m \left(\frac{V_{\text{sep}}}{\omega_0 y_m}(y_m n_z - z_m n_y),\ -z_m,\ y_m \right) \quad . \tag{25}$$

Likewise, with mass ejection constrained to the y-z plane, Eq. 24 becomes

$$\Delta\mathbf{H}_G = (M - m)\omega_0 y_{G'}\ (0,\ -z_{G'},\ y_{G'}) + m\,(V_{\text{sep}}(y_{G'} n_z - z_{G'} n_y),\ 0,\ 0) \quad .$$

Expressing components of $\mathbf{r}_{G'}$ in terms of $\mathbf{r}_m$ allows $\Delta\mathbf{H}_G$ to be reexpressed, by way of Eq. 2, as

$$\Delta\mathbf{H}_G = \frac{m^2}{M-m}\omega_0 y_m \left(\frac{V_{\text{sep}}}{\omega_0 y_m}(y_m n_z - z_m n_y),\ -z_m,\ y_m\right) \quad . \tag{26}$$

We note that, in a fashion analogous to Eq. 8, one may compare Eqs. 25 and 26 to deduce

$$\Delta\mathbf{H}_G = \frac{m}{M-m}\mathbf{H}_m \quad ,$$

such that

$$\mathbf{H}_m + \Delta\mathbf{H}_G = \frac{m\omega_0 y_m}{f}\left(\frac{V_{\text{sep}}}{\omega_0 y_m}(y_m n_z - z_m n_y),\ -z_m,\ y_m\right) \quad ,$$

where we recall from Eq. 9 that $f = (M-m)/M$. With the use of Eq. 23, we arrive, finally, at the angular momentum of the *residual* body, relative to its CG, which is located at G':

$$\mathbf{H}'_{G'} = \frac{m\omega_0 y_m}{f}\left(\frac{V_{\text{sep}}}{\omega_0 y_m}(z_m n_y - y_m n_z),\ \ z_m,\ \ (X-1)y_m\right) \quad , \tag{27}$$

with

$$X = f \cdot \frac{J_s}{m y_m^2} \quad .$$

Here are several nondimensional term groupings to note:

$\dfrac{V_{\text{sep}}}{\omega_0 y_m}$ is the ratio of the normal velocity with which the ejected mass m is being thrown, to its circumferential velocity, at the same moment.

f is the ratio of the residual body mass following the ejection of mass m, to the original body mass.

$\dfrac{J_s}{m y_m^2}$ is the ratio of the original body's moment of inertia about the axis of symmetry, to the moment of inertia of the ejected mass m, relative to the original axis of symmetry.

To summarize, Eq. 27 expresses the angular momentum vector of the residual body, following the ejection of mass m, relative to the residual body's CG, given as G', but in the original (unrotated) x-y-z coordinate system. Consider the origin of the various components of $\mathbf{H}'_{G'}$. Whereas the original spinning body possessed only a

z-component of angular momentum, the ejection of mass m, because of momentum conservation, changes the angular momentum of the residual body in two ways:

- The ejected mass is propelled with an impulse in the y-z plane, which introduces an x component of angular momentum to the residual body.
- The ejected mass (which *a priori* possesses an x-component of linear momentum because of the body's original spin) affects both the y and z angular momentum components of the residual body, proportionally to the z_m and y_m coordinates of the ejected mass, respectively.

3.5 Angular Velocity

To most simply obtain the angular velocity of the residual body, one must first express the angular momentum in the principal orientation of the residual body, rather than the x-y-z orientation. We, thus, wish to express $\mathbf{H}'_{G'}$, given by Eq. 27, along the eigenvectors $\mathbf{T}_1$, $\mathbf{T}_2$, and $\mathbf{T}_3$ (see Eq. 19), which define the residual body's principal axes. This can be accomplished via the method of Eq. 15, to yield

$$\hat{\mathbf{H}} = \mathbb{T}^{\mathrm{T}} \mathbf{H}'_{G'} \tag{28}$$

such that the principal angular momentum components of the residual body, taken about G' in the 1-2-3 coordinate system, may be identified as

$$\begin{aligned} \hat{H}_1 &= \mathbf{T}_1 \cdot \mathbf{H}'_{G'} \\ \hat{H}_2 &= \mathbf{T}_2 \cdot \mathbf{H}'_{G'} \quad . \\ \hat{H}_3 &= \mathbf{T}_3 \cdot \mathbf{H}'_{G'} \end{aligned} \tag{29}$$

The magnitude of angular momentum, which is a time-invariant quantity under torque-free rotation, is given by

$$H = \sqrt{\hat{H}_1^2 + \hat{H}_2^2 + \hat{H}_3^2} \tag{30}$$

and its unit orientation, in the principal 1-2-3 frame of reference,* is given by the

*The corresponding unit orientation of the angular momentum, expressed in the x-y-z laboratory frame, is

$$\mathbf{K} = \left(\frac{H'_{G'x}}{H}, \frac{H'_{G'y}}{H}, \frac{H'_{G'z}}{H} \right) \quad .$$

unit vector $\hat{\mathbf{K}}$ as

$$\hat{\mathbf{K}} = \left(\frac{\hat{H}_1}{H}, \frac{\hat{H}_2}{H}, \frac{\hat{H}_3}{H}\right) \quad . \tag{31}$$

Once the principal components of angular momentum $\hat{H}_i$ are obtained, the angular velocity in this coordinate system, $\hat{\boldsymbol{\omega}}$, follows directly as

$$\begin{aligned} \hat{\omega}_1 &= \hat{H}_1/\lambda_1 \\ \hat{\omega}_2 &= \hat{H}_2/\lambda_2 \quad . \\ \hat{\omega}_3 &= \hat{H}_3/\lambda_3 \end{aligned} \tag{32}$$

The magnitude of the angular velocity is given by

$$\omega = \sqrt{\hat{\omega}_1^2 + \hat{\omega}_2^2 + \hat{\omega}_3^2} \quad . \tag{33}$$

Once the rotational velocity of the residual body is obtained in the principal coordinates of the residual body, the result may be reexpressed in the laboratory coordinate system via $\mathbb{T}$ (Eq. 20):

$$\boldsymbol{\omega} = \mathbb{T}\hat{\boldsymbol{\omega}} \quad . \tag{34}$$

3.5.1 Axisymmetric Simplification to the Angular Velocity

Employing Eqs. 19 and 27, the inner products of Eq. 29 evaluate as

$$\begin{aligned} \hat{H}_1 &= \frac{mV_{\text{sep}}}{f}\big(z_m n_y - y_m n_z\big) \\ \hat{H}_2 &= \frac{m\omega_0 y_m}{f\sqrt{2Q}}\Big(+z_m\sqrt{Q+P} + \operatorname{sgn}(J'_{yz})(X-1)y_m\sqrt{Q-P}\Big) \quad . \\ \hat{H}_3 &= \frac{m\omega_0 y_m}{f\sqrt{2Q}}\Big(-\operatorname{sgn}(J'_{yz})z_m\sqrt{Q-P} + (X-1)y_m\sqrt{Q+P}\Big) \end{aligned} \tag{35}$$

The angular velocity in this coordinate system follows directly from Eq. 32, where λ_i, the eigenvalues, represent the principal moments of inertia of the residual body

While all the equations discussed here apply to the instant following mass ejection, it is the case that $\mathbf{K}$ will also be time-invariant, because of angular-momentum conservation. The same cannot be said of $\hat{\mathbf{K}}$ because, over time, the 1-2-3 body reference frame will vary under precession.

(Eq. 18). Thus, the three rotation rates about the principal axes, $\mathbf{T}_i$, are

$$\begin{aligned}
\hat{\omega}_1 &= \frac{mV_{\text{sep}}}{f} \cdot \frac{z_m n_y - y_m n_z}{J'_{xx}} \\
\hat{\omega}_2 &= \frac{m\omega_0 y_m}{f\sqrt{2Q}} \cdot \frac{z_m\sqrt{Q+P} + \operatorname{sgn}(J'_{yz})(X-1)y_m\sqrt{Q-P}}{J'_{yy} + (Q-P)} \\
\hat{\omega}_3 &= \frac{m\omega_0 y_m}{f\sqrt{2Q}} \cdot \frac{-\operatorname{sgn}(J'_{yz})z_m\sqrt{Q-P} + (X-1)y_m\sqrt{Q+P}}{J'_{zz} - (Q-P)}
\end{aligned} \quad . \tag{36}$$

With the three components of $\hat{\boldsymbol{\omega}}$ available through Eq. 36, the transformation given by Eq. 34 may be used to relocate the angular-velocity vector in the laboratory frame of reference.

4. The Resulting Torque-Free Body Motion

The equations provided in Section 3 allow for the discernment of how the ejection of a small mass m from a spinning axisymmetric body of mass M affects the angular momentum, angular velocity, and principal axes of the body, at a given moment in time. Because the forces of aerodynamic drag and gravity are being neglected in this analysis, one may conclude that, following the mass ejection, the revised angular momentum vector for the residual torque-free body, will remain fixed over time.

One of the ramifications of Eq. 32 is that, for the situation where the angular momentum is perfectly aligned with the body's principal axis, the resulting angular velocity will be, likewise, aligned along the same axis. Conversely, when the angular momentum is not aligned with a principal body axis, the angular velocity vector will, in general, align with neither the angular momentum nor the body's axis. This latter situation brings about the phenomenon of gyroscopic precession, in which the orientation of the body axis, with respect to the laboratory, evolves over time, in a manner that conserves angular momentum.

For prolate axisymmetric bodies (where $J_t > J_s$), the angle (denoted θ) between the original body's z-axis of symmetry and the angular-momentum vector $\mathbf{H}'_{G'}$ will be larger than the angle (denoted γ) between the z-axis of symmetry and the angular velocity $\boldsymbol{\omega}$. When the body is axisymmetric, these three vectors (z-axis, $\mathbf{H}'_{G'}$ and $\boldsymbol{\omega}$) will remain coplanar and a regular precession emerges that is conveniently characterized by what are called the "space cone" and the "body cone", defined in terms of θ and γ.

However, for our problem, we have a complication: *following the ejection of mass m, the residual body is no longer axisymmetric.* The principal axis of the body relocates from the z-axis to the $\mathbf{T}_3$ direction and the principal transverse moments of inertia, λ_1 and λ_2, are no longer co-equal (thus, violating a requirement for axisymmetry). The body's post-ejection motion can no longer be characterized by a simple precession, except in an approximate way. Precession of a non-axisymmetric body is a complex thing. Furthermore, if the angular momentum is primarily aligned with the mid-inertial axis (the axis with neither the largest nor the smallest inertial moment; in our chosen reference frame, the x-axis), then a complex rotational instability arises over time.[2–4]

However, since the ejected mass m has already been assumed to be "small", the transverse moments of inertia of the residual body will be *approximately* co-equal. Thus, the general case may be addressed by way of axisymmetric approximation (with several special cases of initial conditions also examined).

In addition, the conservation of angular momentum and rotational energy is examined for the fully non-axisymmetric case (see the Appendix). Algebraically, it provides the locus and extrema associated with permissible $(\omega_1, \omega_2, \omega_3)$ solutions and the rates of spin $\dot{\psi}$, precession $\dot{\phi}$, and nutation $\dot{\theta}$ (as a function of ψ). It also allows the development of a simple result to determine the precessing axis. Given that the 3-axis, according to the conventions adopted in this report, is loosely associated with the initial z-axis of symmetry of the prolate body, a change of the precessing axis would be a strong indication of rotational instability following the mass ejection. With two simple 1-D integrations to determine the time t and precession angle ϕ in terms of the body's spin, the full precessive behavior of the non-axisymmetric body may be determined.

4.1 Axisymmetric Residual-Body Approximation: $\bar{\lambda}_t = (\lambda_1 + \lambda_2)/2$, with $\hat{\omega}_i = \hat{H}_i/\bar{\lambda}_t$ for $i = 1, 2$

Short of solving the full equations of motion for a non-axisymmetric body in multi-axis torque-free rotation, the easiest way to proceed with the equations of Section 3 is to assume that the residual body is so close to axisymmetry that it can be treated as such. To do so, we must ignore the disparity in moment of inertia between the residual body's 1 and 2 coordinate directions, otherwise given by λ_1 and λ_2, respectively. The way forward here is to assume an aggregated inertia,

$$\bar{\lambda}_t = \frac{\lambda_1 + \lambda_2}{2} \quad , \tag{37}$$

such that Eq. 32 may be approximated as

$$\begin{aligned} \hat{\omega}_1 &\approx \hat{H}_1/\bar{\lambda}_t \\ \hat{\omega}_2 &\approx \hat{H}_2/\bar{\lambda}_t \\ \hat{\omega}_3 &= \hat{H}_3/\lambda_3 \end{aligned} \quad . \tag{38}$$

The level of approximation in Eq. 37 can be characterized by the magnitude

$$\epsilon = \frac{|\lambda_1 - \lambda_2|}{\bar{\lambda}_t} \quad .$$

Once this approximation is made, the problem reduces to axisymmetry where the simple precession solution applies.

There will, however, be an azimuthal discrepancy between the ejection plane and the angular momentum/velocity plane. In the principal 1-2-3 frame of reference, the ejection occurs in the 2-3 plane, whereas the plane in which the resultant momentum and angular velocity lies also contains the 3-axis, but is rotated from the 2-axis toward the 1-axis by an azimuthal angle β_0, such that

$$\tan\beta_0 = \frac{\hat{H}_1}{\hat{H}_2} \quad .$$

The transverse momentum and angular velocity are aggregated as

$$\begin{aligned} \hat{H}_t &= \sqrt{\hat{H}_1^2 + \hat{H}_2^2} \\ \hat{\omega}_t &= \sqrt{\hat{\omega}_1^2 + \hat{\omega}_2^2} \approx \frac{\hat{H}_t}{\bar{\lambda}_t} \end{aligned}$$

Here, $\hat{H}_t$ is introduced to describe the momentum component perpendicular to the prolate axis of the body (*i.e.*, perpendicular to the 3-axis), for our quasi-axisymmetric condition.

Under a condition of axisymmetry, simple precession occurs and the analysis follows the following lines. Referring to Fig. 2, let θ define the angle between the angular momentum and the principal 3-axis, which can be obtained directly in the 1-2-3 frame:

$$\tan\theta = \frac{\hat{H}_t}{\hat{H}_3} \qquad \text{or} \qquad \cos\theta = \hat{K}_3 \quad . \tag{39}$$

For an axisymmetric body, the angle θ represents the invariant angle that exists between the angular momentum vector $\hat{\mathbf{H}}$ (in the laboratory frame, $\mathbf{H}'_{G'}$) and the principal 3-axis, as it precesses around the fixed $\mathbf{H}'_{G'}$.

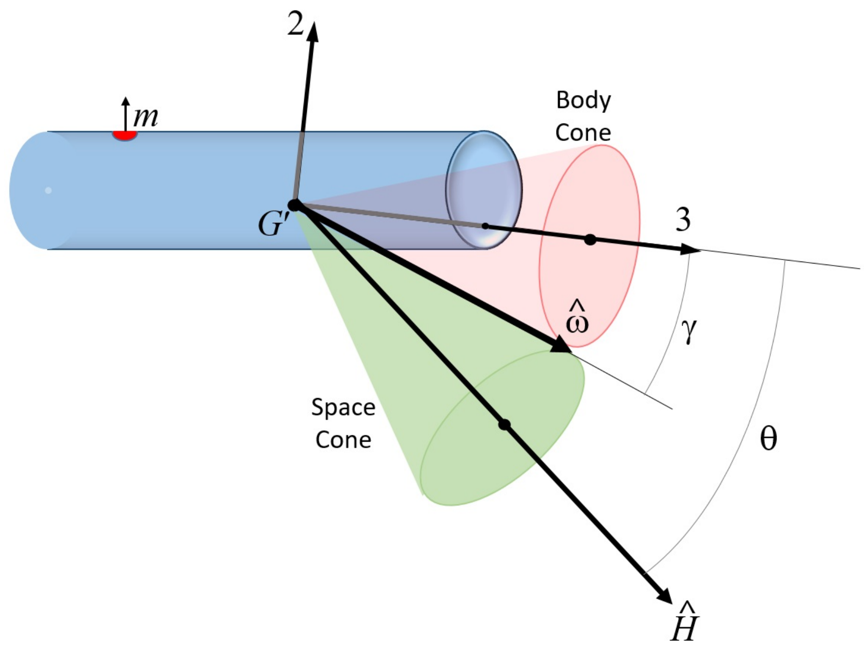

Fig. 2 Precession associated with the residual body under axisymmetric approximation

Let the body-cone angle be denoted as γ, formed between the principal 3-axis and the angular velocity $\boldsymbol{\omega}$. It can be characterized in the principal frame by

$$\tan\gamma = \frac{\hat{\omega}_t}{\hat{\omega}_3} \approx \frac{\hat{H}_t/\bar{\lambda}_t}{\hat{H}_3/\lambda_3} = \frac{\lambda_3}{\bar{\lambda}_t}\tan\theta \quad . \tag{40}$$

The space-cone angle is given by $\theta - \gamma$ and through it, the relations for expressing the rate of precession ($\dot{\phi}$) and the rate of spin ($\dot{\psi}$) emerge in terms of the angular velocity magnitude ($\omega = \sqrt{\hat{\omega}_t^2 + \hat{\omega}_3^2}$, for our case) and the space- and body-cone angles (θ, γ).

Specifically, the triangle formed by the (coplanar) vector sum, $\hat{\boldsymbol{\omega}} = \dot{\phi}\hat{\mathbf{K}} + \dot{\psi}\hat{\mathbf{T}}_3$, through the law of sines, leads directly to

$$\frac{\omega}{\sin\theta} = \frac{\dot{\phi}}{\sin\gamma} = \frac{\dot{\psi}}{\sin(\theta-\gamma)} \quad , \tag{41}$$

from which $\dot{\phi}$ and $\dot{\psi}$ may be calculated. While the precession of the body proceeds at a rate of $\dot{\phi}$, the body spins about its own axis at a rate of $\dot{\psi}$.

One difficulty, however, is that these quantities ($\hat{\boldsymbol{\omega}}$, $\hat{\mathbf{H}}$) are in the principal 1-2-3 reference frame, with nonzero direction cosines connecting them to the laboratory x-y-z frame. Over time, the principal 3-axis precesses with a constant angle θ relative to $\hat{\mathbf{H}}$. But in the laboratory x-y-z reference frame, we wish to know the range of pitch angles experienced by the body relative to the z-axis. The direction cosine between the angular momentum $\mathbf{H}'_{G'}$ and the z-axis, denoted θ_z, remains constant over time. It can be obtained by transforming the angular momentum's direction $\hat{\mathbf{K}}$ from the 1-2-3 frame to the x-y-z frame (see Eq. 16) and extracting the z-component:

$$\cos\theta_z = \mathbb{T}\hat{\mathbf{K}} \cdot (0,\ 0,\ 1) \quad . \tag{42}$$

From the precession, the principal 3-axis of the body maintains an angle of θ with respect to $\mathbf{H}'_{G'}$, so that the angle formed between the laboratory z-axis and the precessing 3-axis will span the range $\theta_z \pm \theta$. Based on geometrical considerations associated with the azimuth (β_0) of angular momentum, one can deduce that θ_z falls in the range $\theta - |\delta| \le \theta_z \le \theta + |\delta|$.

Additionally, in consideration of Eq. 21, the nose of the body will wobble as it spins about its 3-axis by an amount $\pm\delta$ (because of the imbalance brought about by the loss of ejected mass m). Therefore, because of the precession plus wobble, the nose of the body, over time, will gyroscopically pitch to angles covering the range $\theta_z \pm (\theta + |\delta|)$.

4.1.1 Special Cases Arising from Simplified Initial Conditions

There arise certain cases of initial conditions for which the equations of Section 3 can be simplified. In these special cases, certain components of the general problem will be absent, resulting in a simpler result.

4.1.1.1 Rotation-Free Original Body, $\boldsymbol{\omega}_0 \equiv 0$

If the initial body is nonrotational, prior to the mass ejection, such that $\boldsymbol{\omega}_0 \equiv 0$, then the equations of Section 3 are greatly simplified. In particular, the angular momentum in the principal frame of reference, see Eq. 35, consists solely of a single component, brought about by the mass ejection, reexpressed as

$$\hat{H}_1 = \left(mV_{\text{sep}}\right)\left(\frac{z_m}{f}n_y - \frac{y_m}{f}n_z\right) \quad .$$

We see that mV_{sep} is the magnitude of the impulse of the ejected mass m which, from Newton's third law, is the same impulse applied in the opposite direction to the residual body. We note from Eqs. 4 and 9 that $\mathbf{r}_m - \mathbf{r}_{G'} = \mathbf{r}_m/f$. Thus, z_m/f and y_m/f are the distance components of the ejection point with respect to the *revised* (post-ejection) CG of the residual body, G'. The right-hand term in parentheses, therefore, represents a moment arm: the *negative* of $(\mathbf{r}_m + \mathbf{r}_{G'}) \times \mathbf{n}_m$, since the impulse applied to the residual body is equal and *opposite* that imparted to the ejected mass m that is moving in direction $\mathbf{n}_m$. If $\mathbf{r}_m$ and $\mathbf{n}_m$ are parallel, no rotation results ($\hat{H}_1 = 0$), as the impulsive force from the ejection of mass m goes directly through the CG at G'.

Because there is only one principal component of angular momentum for this special case, the angular velocity will be co-aligned with the angular momentum, rotating about the x-axis (since the x- and 1-axes are coincident). Accounting for our axisymmetric approximation, the magnitude of angular velocity will be $\hat{\omega}_1 = \hat{H}_1/\bar{\lambda}_t$ and, because $\hat{\boldsymbol{\omega}}$ is aligned with $\hat{\mathbf{H}}$, the solution represents pure rotation about the x-axis, with no precession whatsoever.

This special case demonstrates how, in a negative way, the absence of initial ω_z body spin fails to provide any stabilization of the body's pitch angle. Here, with no initial spin, the ejection of mass results in a pure tumbling motion of the residual body, reaching eventually 180° of pitch. Additionally, this special case solution represents pure rotation about the mid-inertial axis (the x-axis). If, in the actual situation, small nonzero components of ω_y or ω_z are present, the pure rotation is unstable and will cause these secondary components of ω to grow into a full-fledged precession.

4.1.1.2 Mass Ejected with Zero Normal Velocity, $V_{\text{sep}} \equiv 0$

In the problem as originally described, a mass m, originally in the y-z plane, is ejected from the body. This ejection is accompanied by the exchange of linear momentum in the y-z plane, between the ejected mass and the residual body. This linear momentum absorbed by the residual body will lead to an angular momentum component of the residual body about the x-axis.

One simplified scenario, which results in no-net angular momentum being introduced about the x-axis, occurs when the mass m is ejected with no normal separation velocity, such that $V_{\text{sep}} \equiv 0$. In this scenario, the ejected mass flies off (in a straight line) circumferentially from the spinning body. However, at the moment of separation, there is no net contact force exchange between the ejected mass and the residual body.

Nonetheless, the residual body is no longer strictly axisymmetric, the principal axis formerly aligned with the z-axis is rotated to the $\mathbf{T}_3$ direction, and angular momentum is introduced about the y- and z-axes of the residual body, because of the x-linear momentum removed with the ejected mass m. Looking, however, at Eq. 35, for the case when $V_{\text{sep}} \equiv 0$, it follows that $\hat{H}_1 = 0$ and thus, $\hat{\omega}_1 = 0$.

For this special case, the transverse direction is the 2-axis, such that $\hat{H}_t = \hat{H}_2$. With the help of Eqs. 35 and 39, θ may be obtained as

$$\tan\theta = \frac{\hat{H}_2}{\hat{H}_3} = \frac{+z_m\sqrt{Q+P} + \operatorname{sgn}(J'_{yz})(X-1)y_m\sqrt{Q-P}}{-\operatorname{sgn}(J'_{yz})z_m\sqrt{Q-P} + (X-1)y_m\sqrt{Q+P}} \quad .$$

Note, however, that the principal axis $\mathbf{T}_3$, which precesses about the angular momentum vector $\mathbf{H}'_{G'}$, is no longer aligned with the z-axis. Rather, from Eq. 19, it is offset in the y-z plane by an angle δ, given by Eq. 21. Thus, in the x-y-z coordinates, the angular momentum $\mathbf{H}'_{G'}$ is actually rotated from the z-axis toward the y-axis by an angle $\theta_z = \theta + \delta$. From the precession, the principal 3-axis maintains an angle of θ with respect to $\mathbf{H}'_{G'}$, so that the angle formed between the laboratory z-axis and the precessing 3-axis will span the range $\theta_z \pm \theta$.

As mentioned in the general case, the nose of the body will wobble as it spins about its 3-axis by an amount $\pm\delta$ (because of the imbalance brought about by the loss of ejected mass m). In this special case, however, because the angular momentum is in the 2-3 plane, θ_z can be summed algebraically to $\theta_z = \theta + \delta$ (in lieu of Eq. 42). Thus, during precession, the original nose of the prolate body, forming an angle with respect to the laboratory z-axis of $\theta_z \pm (\theta + |\delta|)$, will span the range from $\delta - |\delta|$ to $2\theta + \delta + |\delta|$.

The components and magnitude of $\hat{\boldsymbol{\omega}}$, under our quasi-axisymmetric assumption, are obtained by way of Eq. 38. The body-cone angle γ can be characterized directly in the 1-2-3 frame using Eq. 40. All the pieces are now in place to calculate the rates of precession and spin:

$$\begin{aligned} \dot{\phi} &= \omega \, \frac{\sin\gamma}{\sin\theta} \\ \dot{\psi} &= \omega \, \frac{\sin(\theta - \gamma)}{\sin\theta} \end{aligned} \quad .$$

While the precession of the body proceeds at a rate of $\dot{\phi}$, the body spins (and thus wobbles) at a rate of $\dot{\psi}$.

4.1.1.3 Negligible Mass Ejected, but with Finite Impulse, $\lim_{m\to 0} mV_{\text{sep}} \equiv P_0$

This special case is formulated a bit differently than the former case. Here, the ejected mass m approaches 0 in the limit; however, it is ejected with such velocity that there is a nonzero impulse interaction between the residual body and the infinitesimal ejection. In essence, this special case is equivalent to the situation of an impulsive load being applied to the original body.

To handle the mathematics of this case, relative to the equations of Section 3, we have the condition that $m = 0$ under the limiting constraint

$$\lim_{m\to 0} mV_{\text{sep}} = P_0 \quad ,$$

where P_0 is the nonzero impulse opposing the outward body normal $\mathbf{n}_m$ at the “ejection site” $\mathbf{r}_m$.

Because the mass ejection is negligible, $g = 0$, the principal moments of the body *do not change*, and the 1-2-3 body coordinate system precisely overlays the x-y-z laboratory system (*i.e.*, $\delta = 0$). Furthermore, the body remains axisymmetric and so the principal axial and transverse moments of inertia remain J_s and J_t, respectively. One immediately concludes that the simple-precession solution applies in this special case.

Let the angular momentum produced by impulse P_0 be defined as

$$H_t = P_0\big(z_m n_y - y_m n_z\big) \quad .$$

Under the conditions of this special case, the angular momentum, originally expressed in Eq. 27, can be greatly simplified as

$$\mathbf{H}'_{G'} = \hat{\mathbf{H}} = \big(H_t,\ 0,\ J_s\omega_0\big) \quad .$$

With $\omega_t = H_t/J_t$, it follows from Eq. 32 that

$$\boldsymbol{\omega} = \big(\omega_t,\ 0,\ \omega_0\big) \quad .$$

For the quantities of precession,

$$\begin{aligned} \tan\theta &= \frac{\hat{H}_t}{\hat{H}_3} = \frac{J_t\,\omega_t}{J_s\,\omega_0} \\ \tan\gamma &= \frac{\hat{\omega}_t}{\hat{\omega}_3} = \frac{J_s}{J_t}\tan\theta = \frac{\omega_t}{\omega_0} \end{aligned} \quad ,$$

and, with some simplification,* the resulting rates of precession and spin may be obtained as

$$\begin{aligned} \dot{\phi} &= \omega\,\frac{\sin\gamma}{\sin\theta} &&= \sqrt{\left(\frac{J_s}{J_t}\,\omega_0\right)^2 + \omega_t^2} \\ \dot{\psi} &= \omega\,\frac{\sin(\theta-\gamma)}{\sin\theta} &&= \omega_0\left(1 - \frac{J_s}{J_t}\right) \end{aligned} \quad .$$

*Recalling the magnitudes of $\hat{\mathbf{H}}$ and $\hat{\boldsymbol{\omega}}$ as H (Eq. 30) and ω (Eq. 33), respectively, then

$$\begin{aligned} \sin\theta &= \frac{J_t\omega_t}{H} \qquad & \cos\theta &= \frac{J_s\omega_0}{H} \\ \sin\gamma &= \frac{\omega_t}{\omega} \qquad & \cos\gamma &= \frac{\omega_0}{\omega} \end{aligned} \quad .$$

Trigonometric substitution yields

$$\sin(\theta-\gamma) = (J_t - J_s)\frac{\omega_0\omega_t}{(H\omega)} \quad .$$

It follows from substitution into Eq. 41 that

$$\dot{\phi} = \frac{H}{J_t} \qquad \dot{\psi} = \omega_0\frac{J_t - J_s}{J_t} \quad .$$

A final reduction gives the results that follow in the report.

Since the applied impulse P_0 was in the y-z plane, no additional rotational inertia was added about the z axis, and so the rate of spin, $\dot{\psi}$ is unaffected by P_0 (*i.e.*, unaffected by ω_t). During precession, the total body pitch will vary over the range of $[0, 2\theta]$.

4.2 Energy/Momentum Analysis of Torque-Free Rotation

Once the ejection of mass occurs, the residual body is no longer subject to any forces and, therefore, is in a condition to conserve energy and momentum. Since the body travels inertially following the ejection with a velocity of $\mathbf{V}_{G'}$, there is *a priori* no change in linear momentum nor kinetic energy. Therefore, in the absence of kinetic exchange, the angular momentum and rotational energy are likewise conserved.

In the case of momentum, since the vector $\mathbf{H}'_{G'}$ is fixed over time, it is also the case that the scalar $H^2 = \mathbf{H}'_{G'} \cdot \mathbf{H}'_{G'} = \hat{\mathbf{H}} \cdot \hat{\mathbf{H}}$, representing the square of the angular momentum magnitude, is also a fixed quantity, regardless of the reference frame in which it is expressed. From Eqs. 30 and 32,

$$\lambda_1^2 \hat{\omega}_1^2 + \lambda_2^2 \hat{\omega}_2^2 + \lambda_3^2 \hat{\omega}_3^2 = H^2 = \text{constant} \quad . \tag{43}$$

A tabulation of rotational kinetic energy T_{rot}, which also remains fixed, gives

$$\lambda_1 \hat{\omega}_1^2 + \lambda_2 \hat{\omega}_2^2 + \lambda_3 \hat{\omega}_3^2 = 2T_{\text{rot}} = \text{constant} \quad . \tag{44}$$

In graphical terms, using a 3-D space comprising $\hat{\omega}_i$-$\hat{\omega}_j$-$\hat{\omega}_k$ axes, Eqs. 43 and 44 represent two ellipses, centered at the origin and aligned with the coordinate axes.[3] The surface of each ellipse represents the permissible values of the $(\hat{\omega}_1, \hat{\omega}_2, \hat{\omega}_3)$ triplet that satisfy the conservation of angular momentum and rotational energy, respectively. Therefore, all possible rotational states that conserve *both* angular momentum and rotational energy over time are represented by the intersection of the two ellipses.

We know the values of λ_i for our residual body by way of Eq. 18. Likewise, Eq. 36 provides the initial values of $\hat{\omega}_i$ immediately following the mass ejection. Therefore, the conservation quantities, H^2 and $2T_{\text{rot}}$, follow immediately from an application of Eqs. 43 and 44 to this initial state. A closed-form solution to the intersection of these two ellipses has presented itself—the method used to ascertain that intersection is described in the Appendix.

In the simple precession solution associated with axisymmetric bodies, the elliptical intersection is given by a circle perpendicular to the $\hat{\omega}_3$ axis, so that $\hat{\omega}_3$ remains fixed. The radius of the circle is $\hat{\omega}_t = \sqrt{\hat{\omega}_1^2 + \hat{\omega}_2^2}$. The body-cone angle γ (which in this case is represented by the conical angle that connects the circle of intersection to the origin) is fixed at $\gamma = \tan^{-1}(\hat{\omega}_t / \hat{\omega}_3)$.

For the *non-axisymmetric* case of elliptical intersection, quantities like $\hat{\omega}_3$ and γ are no longer fixed, but will vary through the precession cycle. For small deviations of the residual body from axisymmetry, the variations of $\hat{\omega}_3$ and γ about nominal values remain small. These variations increase as the deviation from axisymmetry grows. If the axisymmetric deviation grows large enough, an interesting result happens: *the precessing axis shifts from the 3-axis to either the 1- or 2-axes.*

One may define the precessing axis i as that axis for which no $\hat{\omega}_i = 0$ solution exists. By exercising the model presented in the Appendix, the analytical condition to determine the precessing axis was inferred. It proves so simple, that one need not actually exercise the model to ascertain the precessing axis. For ease of explanation, let us denote and order the three principal moments as

$$\lambda_{\text{min}} < \lambda_{\text{mid}} < \lambda_{\text{max}} \quad .$$

The criterion to determine the precessing axis is simply

$$\text{if } \frac{H^2}{2T_{\text{rot}}} \begin{cases} > \lambda_{\text{mid}}, & \text{the precessing axis is that associated with } \lambda_{\text{max}} \\ < \lambda_{\text{mid}}, & \text{the precessing axis is that associated with } \lambda_{\text{min}} \\ = \lambda_{\text{mid}}, & \text{the rotation is unstable} \end{cases} \quad . \tag{45}$$

Consider the hypothetical situation provided in Table 1, in which the range of $(\hat{\omega}_1, \hat{\omega}_2, \hat{\omega}_3)$ solutions are presented for a residual body, for a given initial rotation rate, subject to successive excursions of lesser λ_1. In essence, each row of the table represents a case further removed from the condition of axisymmetry. The critical value of λ_1 (where $\hat{\omega}_3$ first reaches 0) proves to be 2.753 $\left(\text{when } \lambda_1 = \frac{H^2}{2T_{\text{rot}}}\right)$, below which the 2-axis becomes the precessive axis. While the axisymmetric body cone (the angle between the prolate axis and the angular velocity) angle γ remains fixed at $19.8°$, as asymmetry is introduced (through $\lambda_1 \neq \lambda_2$), the maximum value of γ grows rapidly until reaching $90°$ at the critical value of λ_1.

Table 1 Precession range for the hypothetical initial condition of $(\hat{\omega}_1, \hat{\omega}_2, \hat{\omega}_3) = (0.2, 0.3, 1.0)$, under the effect of reducing the principal moment λ_1

λ_1	λ_2	λ_3	$\frac{H^2}{2T_{\mathrm{rot}}}$	$\hat{\omega}_3$ **range**	γ **range** $(^\circ)$	θ **range** $(^\circ)$
6	6	1	3.19	1.00	19.8	65.2
5.7	6	1	3.13	0.98–1.01	19.4–20.9	64.7–65.3
5.4	6	1	3.08	0.96–1.01	19.0–22.2	64.2–65.6
5	6	1	3.01	0.93–1.02	18.5–24.2	63.5–66.0
4	6	1	2.87	0.80–1.03	17.5–32.8	62.2–68.8
3	6	1	2.77	0.44–1.04	16.8–58.1	61.1–78.3
2.753	6	1	2.75	**0.00**–1.04	16.7–90.0	61.0–90.0
2	6	1	2.72	0.00–1.03	16.4–90.0	60.5–90.0

The cases represented in Table 1 are presented graphically in Fig. 3. The moment of inertia that permits $\gamma = 90^\circ$, conversely $\hat{\omega}_3 = 0$, represents a body geometry for which the precessing axis has shifted away from the 3-axis. One may observe that for the condition $\lambda_1 < 2.753$, there exist ψ configurations for which no ω_3 solutions exist, implying that precession is no longer about the 3-axis. The greater the divergence from axisymmetry, the larger the fluctuation in both γ and the body spin rate, $\hat{\omega}_3$. The abscissa ψ represents the body's angular coordinate of spin.

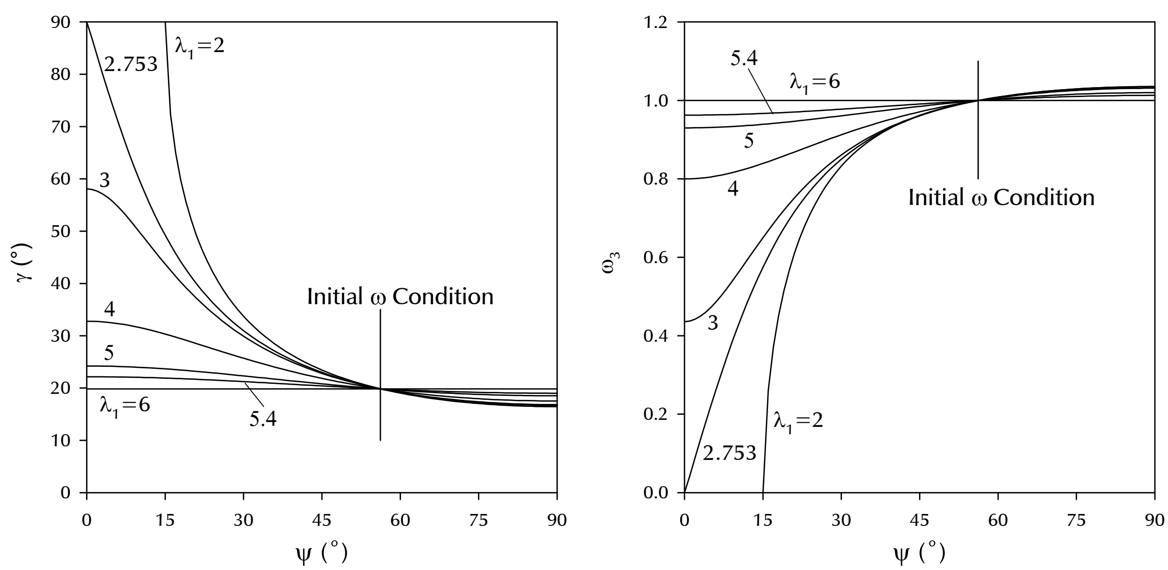

(a) **(b)**

Fig. 3 Locus of solutions for bodies with an initial angular velocity $\hat{\omega} = (0.2, 0.3, 1)$, with moment-of-inertia component λ_1 as a parameter, depicting (a) γ and (b) $\hat{\omega}_3$

On the other hand, when λ_1 undergoes a 10% decrease to a value of 5.4, the effect is quite small, with $\hat{\omega}_3$ only fluctuating 5% and γ spanning a range of 3.2° about its nominal (axisymmetric) value. The solution for $\lambda_1 = 5.4$ is shown in Fig. 4. So, the initial sensitivity to small variations in λ_i, owing to the ejection of mass m, may still remain quite small, even as 5% or 10% of the body mass is ejected. This result gives confidence to the earlier solution involving axisymmetric approximation. Of course, the particulars will depend on the inertia of the original body and the level of change in angular momentum brought about by the ejection of mass.

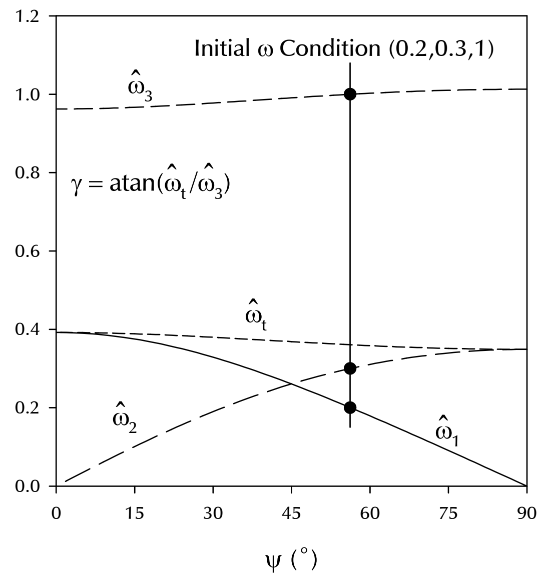

Fig. 4 Locus of $\hat{\omega}$ solutions for body with principal moments $(5.4, 6, 1)$, subject to the initial condition. The term $\psi = \tan^{-1}\xi$ is the implicit variable in the solution (see the Appendix).

The transformation matrix $\mathbb{T}$, given in Eq. 20, from which the orientation of the body's principal axes can be derived, is valid only for the instant following the ejection of mass m. Once the torque-free rotation is allowed to proceed, the residual body's orientation, and thus $\mathbb{T}$ and $\hat{\mathbf{H}}$, also evolve in time. In the axisymmetric case, the body and space cones are of fixed angle. Thus the locus of body orientations is known through the precession cycle. However, this is not the case for non-axisymmetry.

The energy approach presented in the Appendix provides the locus of $\hat{\boldsymbol{\omega}}$ (and $\hat{\mathbf{H}}$, by way of Eq. 32) that evolve during the precession. Despite a promising avenue, however, there would appear to be no way to use that information to back out the body's instantaneous orientation embodied in the $\mathbb{T}$ matrix. We know that each of these $\hat{\mathbf{H}}$ triplets, over the range of solutions, is equivalent to the known $\mathbf{H}'_{G'}$ vector (Eq. 27) that is fixed in the x-y-z coordinate system. There exists a technique,[5] for a given $\hat{\mathbf{H}}$ triplet, to obtain a transform $\mathbb{R}$ that connects it to $\mathbf{H}'_{G'}$ in the laboratory coordinates.* Unfortunately, in 3-D, that transform is not unique and therefore it cannot serve as a general approach for back-calculating $\mathbb{T}$ given $\hat{\mathbf{H}}$ and $\mathbf{H}'_{G'}$.

Nonetheless, the knowledge of the locus of $\hat{\mathbf{H}}$ does provide for the possible range of residual-body orientations. That is to say, while not knowing the actual 1-2-3 coordinate axes at any given moment in the torque-free precession, knowledge of $\hat{\mathbf{H}}$ allows for the direction cosine between the angular momentum and the body axis to be obtained by way of θ, Eq. 39. Therefore, the minimum and maximum values of θ over the full locus of $\hat{\mathbf{H}}$ solutions will define two cones centered around the angular momentum vector, $\mathbf{H}'_{G'}$. The actual orientation of the residual body's prolate axis must fall between the rims of these two cones at all times during the precession.

---

*Applying the cited approach to our current situation, we draw upon the (fixed) $\mathbf{K}$ and the (time varying) $\hat{\mathbf{K}}$, which both represent the unit orientation of the fixed angular momentum vector, respectively expressed in the laboratory and the principal (body) coordinate systems (see Eq. 31). Let $\mathbf{Q} = \hat{\mathbf{K}} \times \mathbf{K}$ and $c = \hat{\mathbf{K}} \cdot \mathbf{K}$. Defining $\mathbb{Q}_\times$ as the skew-symmetric cross product of vector $\mathbf{Q}$,

$$\mathbb{Q}_\times = \begin{bmatrix} 0 & -Q_z & Q_y \\ Q_z & 0 & -Q_x \\ -Q_y & Q_x & 0 \end{bmatrix} \quad ,$$

there exists *a* rotational transformation matrix $\mathbb{R}$, which may be expressed (except for the degenerate case when $\hat{\mathbf{K}} = -\mathbf{K}$) as

$$\mathbb{R} = \mathbf{I} + \mathbb{Q}_\times + \frac{1}{1+c}\mathbb{Q}_\times^2$$

But is $\mathbb{R}$ unique? The columns of $\mathbb{R}$ (recall Eq. 14) are the vectors composing the transformed 1-2-3 coordinate system, expressed in the laboratory x-y-z frame of reference. Thus, the equation provides the means, given a $(\hat{\omega}_1, \hat{\omega}_2, \hat{\omega}_3)$ triplet, to obtain *an* associated coordinate system. Unfortunately, in 3-D, that transform $\mathbb{R}$ is not unique and therefore there is no guarantee, as might have been hoped, that $\mathbb{R} \equiv \mathbb{T}$.

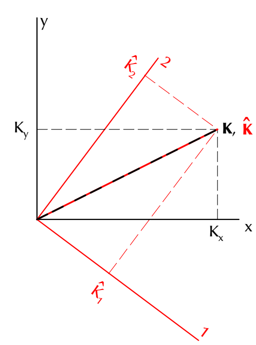

The schematic shows $\mathbf{K}$ and $\hat{\mathbf{K}}$ as the unit orientation of the fixed momentum vector, but respectively expressed in the fixed x-y-z laboratory frame (black) and the precessing 1-2-3 body frame (red). Note that the z- and 3-coordinate axes (not shown) are perpendicular to page. Because, in 3-D, the red 1-2-3 coordinate frame is not unique (others can be acquired by rotating it about the $\hat{\mathbf{K}}$ axis), the goal of acquiring $\mathbb{T}$, solely given $\mathbf{K}$ and $\hat{\mathbf{K}}$, is not possible.

For example, using the rotation described in Fig. 4, after reconstituting $\hat{H}_i = \lambda_i \hat{\omega}_i$, the initial condition sets $\theta_0 = 64.5°$ and the solution, over the full cycle of precession, provides the range of θ as $64.2°$–$65.6°$.

4.3 A Full Example

We here endeavor to combine all the aspects derived in this report into one representative example. The example starts with a spinning axisymmetric body of a given description and then specifies the mass-ejection event. The equations of this report are employed to track the resulting effect on the body's motion.

Consider an initially axisymmetric body of $M = 10\,\mathrm{kg}$, spinning about the z-axis of symmetry at $\omega_0 = 30\,\mathrm{rad\,s^{-1}}$ (4.77 rps), whose moment of inertia is described by Eq. 1, with $J_t = 6\,\mathrm{kg\,m^2}$ and $J_s = 1\,\mathrm{kg\,m^2}$, so that

$$\mathbf{J}_G = \begin{bmatrix} 6 & 0 & 0 \\ 0 & 6 & 0 \\ 0 & 0 & 1 \end{bmatrix} \mathrm{kg\,m^2} \quad .$$

The initial angular velocity and angular momentum vectors are

$$\boldsymbol{\omega} = (0,\ 0,\ 30)\,\mathrm{rad\,s^{-1}} \qquad \mathbf{H} = \mathbf{J}_G \boldsymbol{\omega} = (0,\ 0,\ 30)\,\mathrm{kg\,m^2/s} \quad .$$

We use the mks unit system throughout this example.

At an instant in time, the body undergoes an impulsive mass ejection of $m = 1\,\mathrm{kg}$, originating from the location $\mathbf{r}_m = (0,\ 0.5,\ -1)\mathrm{m}$ (*i.e.*, $1\,\mathrm{m}$ aft of the CG, at a radius of $0.5\,\mathrm{m}$). The ejected mass is expelled at a velocity of $V_{\mathrm{sep}} = 10\,\mathrm{m/s}$ in a radial direction (normal to the surface), $\mathbf{n}_m = (0,\ 1,\ 0)$.

The fraction of mass ejected, from Eq. 3, is $g = 0.1$. The CG shifts in the residual body, in accordance with Eq. 4, by an amount $\mathbf{r}_{G'} = (0.,\ -0.0556,\ 0.1111)\,\mathrm{m}$. From conservation of linear momentum, Eq. 5, the velocity of the ejected mass is $\mathbf{V}_m = (-15,\ 9,\ 0)\,\mathrm{m/s}$ and that of the residual body is $\mathbf{V}_{G'} = (1.6667,\ -1,\ 0)\,\mathrm{m/s}$.

The complement of g is given by Eq. 9 as $f = 0.9$. The moment of inertia of the residual body in the x-y-z frame, accounting for both the mass ejection as well as the shift in the CG, is given by Eq. 11, as

$$\mathbf{J}'_{G'} = \begin{bmatrix} 4.6111 & 0 & 0 \\ 0 & 4.8889 & -0.5 \\ 0 & -0.5 & 0.7222 \end{bmatrix} \mathrm{kg\,m^2} \quad .$$

In transforming to the principal coordinate 1-2-3 frame, we obtain the intermediate result that $P = 2.0833\,\mathrm{kg\,m^2}$ and $Q = 2.1425\,\mathrm{kg\,m^2}$, so that, from Eq. 18,

$$\hat{\mathbf{J}} = \begin{bmatrix} \lambda_1 & 0 & 0 \\ 0 & \lambda_2 & 0 \\ 0 & 0 & \lambda_3 \end{bmatrix} = \begin{bmatrix} 4.6111 & 0 & 0 \\ 0 & 4.9480 & 0 \\ 0 & 0 & 0.6631 \end{bmatrix} \mathrm{kg\,m^2} \quad .$$

From this result, the rotational transformation matrix may be obtained as the eigenvectors of λ_i, according to Eq. 20:

$$\mathbb{T} = \begin{bmatrix} 1 & 0 & 0 \\ 0 & 0.9931 & 0.1175 \\ 0 & -0.1175 & 0.9931 \end{bmatrix} \quad .$$

The three columns of $\mathbb{T}$ represent the 1, 2, and 3 principal-axis vectors, respectively, of the residual body, in the moment following the mass ejection. From Eq. 21, we note that the prolate 3-axis has shifted from the z-axis toward the y-axis by an amount $\delta = 6.75°$.

Calculating the $X = 3.6$, we employ Eq. 27 to obtain the angular momentum of the residual body in the laboratory coordinates as

$$\mathbf{H}'_{G'} = (-11.1111,\ -16.6667,\ 21.6667)\,\mathrm{kg\,m^2/s} \quad .$$

This angular momentum, in the absence of outside torques, will be invariant over time. It may be transformed to the principal 1-2-3 coordinates by way of Eq. 28:

$$\hat{\mathbf{H}} = (-11.1111,\ -19.0971,\ 19.5582)\,\mathrm{kg\,m^2/s} \quad .$$

Unlike $\mathbf{H}'_{G'}$, the quantity $\hat{\mathbf{H}}$ will change as the principal coordinate system precesses over time. However, its magnitude H (Eq. 30) will remain fixed at $H = 29.5073\,\mathrm{kg\,m^2/s}$.

In the immediate aftermath of the mass ejection, The unit orientation of $\hat{\mathbf{H}}$, the angular momentum in the body frame, is given by

$$\hat{\mathbf{K}} = (-0.3766,\ -0.6472,\ 0.6628) \quad .$$

The initial angle between the angular momentum vector and the principal 3-axis, may be obtained from Eq. 39 as $\theta_0 = 48.48°$. Likewise, the angle between the angular momentum vector and the laboratory z-axis, from Eq. 42, is $\theta_z = 42.75°$. This latter quantity will be time invariant.

At this point, one may proceed in two directions: approximate the residual body as axisymmetric, or retain the non-axisymmetric character of the solution.

4.3.1 Axisymmetric Approximation

If the residual body of our example is to be approximated in an axisymmetric fashion, things simplify greatly. The value of θ, initially equal to θ_0, will not vary under the regular precession of axisymmetry. Thus, $\theta = 48.48°$, the angle between the momentum vector and the 3-axis, remains a fixed quantity under precession. The principal moments in the 1-2 plane are averaged by way of Eq. 37 to re-acquire an axisymmetric configuration, so that $\bar{\lambda}_t = 4.7796\,\mathrm{kg\,m^2}$. This value of $\bar{\lambda}_t$ is used to approximate both λ_1 and λ_2, so that the axisymmetric approximation of the angular velocity vector may be obtained from Eq. 38 as $\hat{\boldsymbol{\omega}} \approx (-2.3247,\ -3.9956,\ 29.4968)\,\mathrm{rad\,s^{-1}}$. Under the axisymmetric assumption, its magnitude will remain fixed at $29.8569\,\mathrm{rad\,s^{-1}}$. Further, the $\hat{\omega}_3$ component will also remain fixed, while the $\hat{\omega}_1$ and $\hat{\omega}_2$ components vary sinusoidally with the body spin.

The angle between the principal axis of the body and the (approximated) angular velocity vector, given in Eq. 40, remains fixed at $\gamma = 8.91°$. The fixed rates of precession and spin are given, respectively, as $\dot{\phi} = 6.1736\,\mathrm{rad\,s^{-1}}$and $\dot{\psi} = 25.4048\,\mathrm{rad\,s^{-1}}$, as dictated by Eq. 41. The time to precess one complete cycle about the momentum vector is simply $2\pi/\dot{\phi} = 1.02\,\mathrm{s}$.

The angle formed between the laboratory z-axis and the precessing 3-axis will span the range $\theta_z \pm \theta = 42.75° \pm 48.48°$. Additionally, in consideration of Eq. 21, the nose of the body will wobble as it spins about its 3-axis by an amount $\pm\delta$ (because of the imbalance brought about by the loss of ejected mass m). Therefore, because of the precession plus wobble, the nose of the body, over time, will gyroscopically pitch to angles covering the range $\theta_z \pm (\theta + |\delta|) = 42.75° \pm 55.23°$, resulting in a maximum pitch of $97.98°$.

4.3.2 Non-Axisymmetry Retained

In the absence of an axisymmetric approximation, one may call upon the energy conservation approach described in the Appendix. When not approximating $\hat{\mathbf{J}}$ into an axisymmetric configuration, the precise measure of angular velocity, immediately following the ejection of mass m, is obtained directly from Eq. 32 as $\hat{\boldsymbol{\omega}} = (-2.4096,\ -3.8595,\ 29.4968)\,\mathrm{rad\,s^{-1}}$. The magnitude of $\hat{\boldsymbol{\omega}}$ (Eq. 33) is calculated as $\omega = 29.8457\,\mathrm{rad\,s^{-1}}$. The initial value of γ, denoting the momentary angle between the 3-axis and the angular velocity vector immediately after mass ejection, is $\gamma_0 = 8.77°$ (Eq. 40). At this initial moment following the mass ejection, the angular velocity $\hat{\boldsymbol{\omega}}$ is oriented at an azimuth of $\psi_0 = 58.02°$ from the 1-axis (in the 1-2 plane), in accordance with Eq. A-1 (using the $ijk = 123$ triplet).

The energy and angular momentum quantities to conserve, given in Eq. 43 and 44, are $H^2 = 870.7\,\mathrm{kg^2\,m^4\,s^{-2}}$ and $2T_{\mathrm{rot}} = 677.4\,\mathrm{J}$, such that $\frac{1}{2}H^2/T_{\mathrm{rot}} = 1.29\,\mathrm{kg\,m^2}$. Based on the stability criterion, Eq. 45, we conclude that that the 3-axis remains the precessing axis. The methods described in the Appendix are applied and presented in Table 2.

Table 2 Locus of $\hat{\omega}$ as a function of ψ, with $\hat{\omega} = (-2.4096, -3.8595, 29.4968)$ rad s^{-1}as part of the solution, with $(\lambda_1, \lambda_2, \lambda_3) = (4.6111, 4.9480, 0.6631)$ kg m^2

ψ (°)	ξ	$\pm\hat{\omega}_1$ (s^{-1})	$\pm\hat{\omega}_2$ (s^{-1})	$\pm\hat{\omega}_3$ (s^{-1})	γ (°)	θ (°)	$\dot{\psi}$ (s^{-1})	$\dot{\phi}$ (s^{-1})	$\dot{\theta}$ (s^{-1})
90.0	∞	0.0000E+00	4.4588E+00	2.9551E+01	8.58	48.39	25.59	5.96	0.00
80.0	5.6713E+00	7.7592E−01	4.4005E+00	2.9545E+01	8.60	48.40	25.57	5.98	−0.07
70.0	2.7475E+00	1.5378E+00	4.2250E+00	2.9529E+01	8.66	48.43	25.54	6.01	−0.13
60.0	1.7321E+00	2.2699E+00	3.9316E+00	2.9503E+01	8.75	48.47	25.48	6.06	−0.18
50.0	1.1918E+00	2.9536E+00	3.5200E+00	2.9470E+01	8.86	48.53	25.41	6.13	−0.21
40.0	8.3910E−01	3.5668E+00	2.9929E+00	2.9433E+01	8.99	48.59	25.33	6.20	−0.22
30.0	5.7735E−01	4.0840E+00	2.3579E+00	2.9396E+01	9.11	48.66	25.24	6.28	−0.20
20.0	3.6397E−01	4.4788E+00	1.6301E+00	2.9364E+01	9.22	48.71	25.18	6.34	−0.15
10.0	1.7633E−01	4.7271E+00	8.3351E−01	2.9343E+01	9.29	48.75	25.13	6.38	−0.08
0.0	0.0000E+00	4.8119E+00	0.0000E+00	2.9336E+01	9.32	48.76	25.12	6.40	0.00

From the results, it is seen that, unlike the solution with approximated axisymmetry, where γ and θ remain fixed at $\gamma = 8.91°$ and $\theta = 48.48°$, the energy conservation solution reveals a range on these quantities. In particular, γ spans the range $8.58°$–$9.32°$ while θ spans $48.39°$–$48.76°$. To pursue this general approach to its conclusion, the nose of the body will pitch, through the course of its precession, to cover the range $\theta_z \pm (\theta_{\text{max}} + |\delta|) = 42.75° \pm 55.51°$, resulting in a maximum pitch of $98.26°$.

Unlike Fig. 3, which showed the large extent to which the precession parameters could change with a significant mass ejection, this example problem highlights the other end of the spectrum, in which the axisymmetric approximation seems well justified. A graphical comparison between the full solution and the axisymmetric approximation is given in Fig. 5.

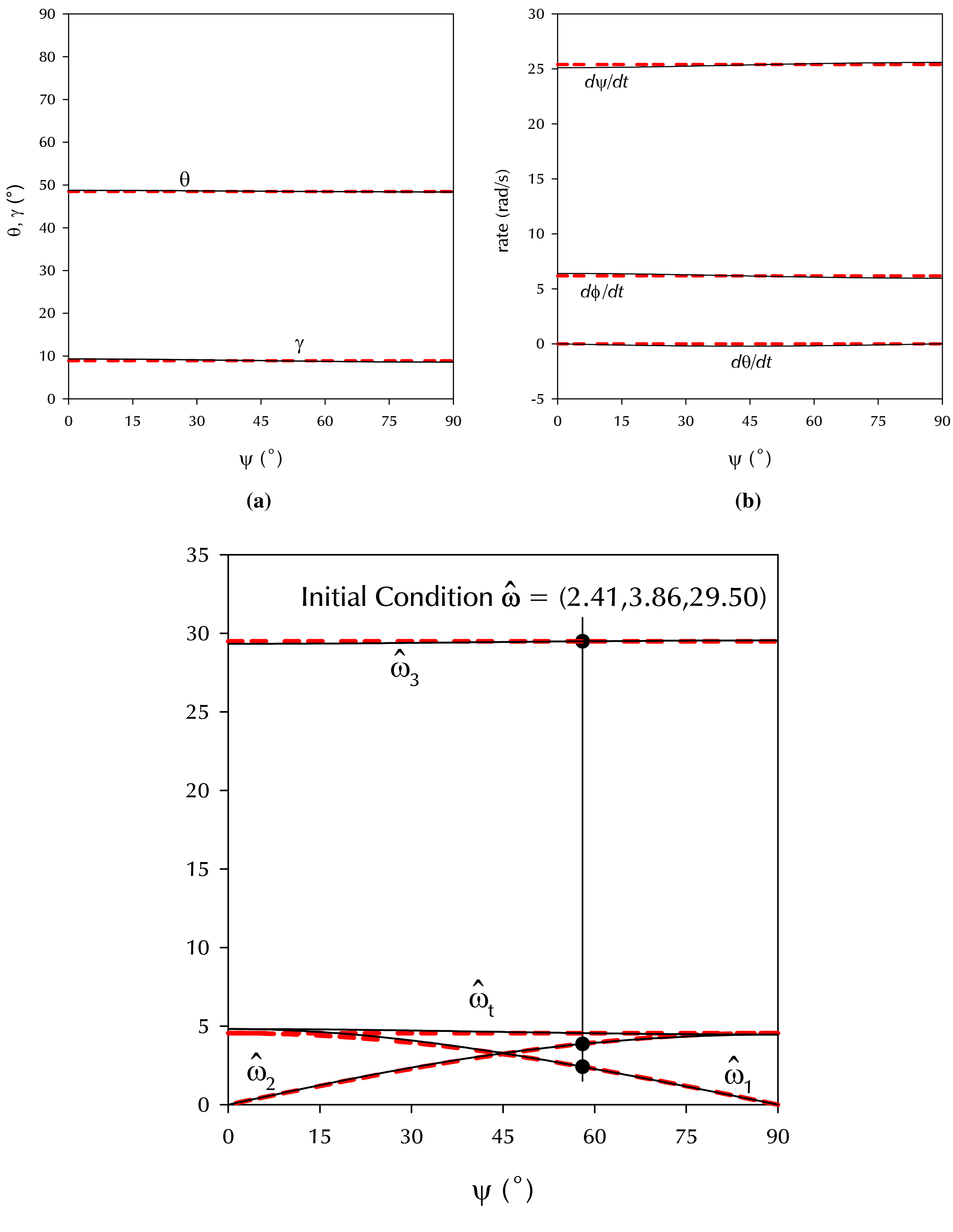

Fig. 5 Considered example with the full solution in black and the axisymmetric approximation in dashed red, for (a) θ, γ, (b) $\dot{\psi}$, $\dot{\phi}$, $\dot{\theta}$, and (c) $\hat{\omega}$

5. Conclusion

In this report, a rigid-body-dynamics analysis was performed on a body, free of gravity and aerodynamic forces, initially spinning about its axis of symmetry, subject to a small but impulsive ejection of mass normal to its surface. The effect of mass loss and CG shift are considered when deriving the residual body's moment of inertia and angular momentum. Relations to achieve coordinate rotation between the laboratory frame of reference and the residual body's principal frame are derived, so that the angular velocity and the parameters associated with precessive motion may be simply obtained. These relations are further used to relate the precession (derived in the principal coordinate frame) back to the laboratory coordinates, so that the range of resultant pitch/yaw angles may be formulated.

The problem's complexity increases, since the residual body, following the ejection of surface mass, is no longer axisymmetric. In approximating the residual body as axisymmetric, several constrained special cases are considered. In addition, for the general case of the residual body subject to triaxial rotation, a quasi-axisymmetric assumption may be introduced to facilitate a solution that is still governed by the classical solution of simple precession.

Importantly, however, a non-axisymmetric algebraic solution is also provided for the evolution of the precessing body. Because the approach employs conservation of energy, the time dependence is not part of the algebraic solution. However, the full locus of $(\hat{\omega}_1,\, \hat{\omega}_2,\, \hat{\omega}_3)$ solutions (in the body coordinates) are obtained. In addition, the rates of residual-body spin $\dot{\psi}$, precession $\dot{\phi}$, and nutation $\dot{\theta}$ (in the principal coordinates) can be algebraically calculated as a function of body orientation ψ.

With this information, it becomes trivial to employ $\dot{\psi}$ as a function of ψ to numerically integrate for the time dependence. Likewise, the precession ϕ (as a function of ψ or t) can be simply recovered in a similar manner. With this added bit of time-dependent information $(\phi(t), \psi(t), \theta(t))$ acquired through integration, it is sufficient to provide the laboratory-frame body orientation history. Even without the added time dependence, the algebraic solution provides the range of motion of the precessing axis, which can be used to place limits on the body's laboratory-frame orientation during the precessive motion.

6. References

1. Beer FP, Johnston Jr ER. Vector mechanics for engineers: dynamics. 3rd ed. New York (NY): McGraw Hill; 1977. (Chapter 18: Kinematics of Rigid Bodies in Three Dimensions).

2. Garriott R. Richard Garriott space video blog: rotational inertia. Washington (DC): Challenger Center for Space Science Education; 2009 Mar 11 [accessed 2018 May 25]. https://www.youtube.com/watch?v=fPI-rSwAQNg.

3. Fowles GR, Cassiday GL. Analytical mechanics. New York (NY): Saunders College Publishing; 1999.

4. Goldstein H, Poole C, Safko J. Classical mechanics. San Francisco (CA): Addison Wesley; 2002.

5. van den Berg J. Calculate rotation matrix to align vector a to vector b in 3d? Gent (Belgium): Stack Overflow; 2013 Aug 26 [accessed 2018 June 22]. https://math.stackexchange.com/questions/180418/calculate-rotation-matrix-to-align-vector-a-to-vector-b-in-3d.

Appendix. Momentum/Energy Approach in Solving the Precession of a Non-Axisymmetric Body

In Eqs. 43 and 44, repeated here for convenience, conservation of angular momentum and rotational energy are expressed for the problem of torque-free rotation:

$$\lambda_1^2\hat{\omega}_1^2 + \lambda_2^2\hat{\omega}_2^2 + \lambda_3^2\hat{\omega}_3^2 = H^2 \quad = \text{constant} \tag{43}$$

$$\lambda_1\hat{\omega}_1^2 + \lambda_2\hat{\omega}_2^2 + \lambda_3\hat{\omega}_3^2 = 2T_{\text{rot}} = \text{constant} \tag{44}$$

The conservation quantities H and T_{rot} are available through the substitution of the principal moments λ_i (Eq. 18), and $\hat{\omega}_i$ (Eq. 36), which are the angular velocity components in the residual-body 1-2-3 coordinate system, in the instant following mass ejection.

A.1 Elliptical Intersection

If one employs a 3-D angular-velocity space comprising the $\hat{\omega}_1$-$\hat{\omega}_2$-$\hat{\omega}_3$ axes, Eqs. 43 and 44 represent two ellipses, centered at the origin and aligned with the coordinate axes. The surface of each ellipse represents the permissible values of the $(\hat{\omega}_1,\, \hat{\omega}_2,\, \hat{\omega}_3)$ triplet that satisfies conservation of angular momentum and rotational energy, respectively. Therefore, all possible rotational states that conserve *both* angular momentum and rotational energy over time are represented by the intersection of the two ellipses.[1] We need only solve the elliptical intersection in the 1st octant, because of symmetry.

The following derivation applies to any principal-coordinate triplet ijk (*i.e.*, 123, 231, or 312), but is derived with the *a priori* presumption (but not guarantee) that it is the k-axis, which precesses about the angular momentum vector. In the pure axisymmetric case, with the axis of symmetry aligned with the body's k-axis, the elliptical intersection is two circles perpendicular to the $\hat{\omega}_k$-axis, symmetric across the $\hat{\omega}_i$-$\hat{\omega}_j$ plane, whose centers falls upon the $\hat{\omega}_k$-axis. The k-axis is the precessing axis *precisely because* the elliptical intersection circumnavigates the $\hat{\omega}_k$-axis but not the other axes. Since our problem represents a deviation from this very situation, we choose as the independent variable the azimuthal angle ψ that lies in the $\hat{\omega}_i$-$\hat{\omega}_j$ plane, such that

$$\tan\psi = \xi = \frac{\hat{\omega}_j}{\hat{\omega}_i} \quad . \tag{A-1}$$

As the azimuth ψ varies from 0 to $\pi/2$, ξ will vary from 0 to ∞. Equation A-1 may

[1]Fowles GR, Cassiday GL. Analytical mechanics. New York (NY): Saunders College Publishing; 1999.

be substituted into Eqs. 43 and 44, to eliminate $\hat{\omega}_j$:

$$\begin{aligned} A\hat{\omega}_i^2 + \lambda_k^2\hat{\omega}_k^2 &= H^2 \\ B\hat{\omega}_i^2 + \lambda_k\hat{\omega}_k^2 &= 2T_{\text{rot}} \end{aligned} \quad , \tag{A-2}$$

where

$$\begin{aligned} A(\xi) &= \lambda_i^2 + \xi^2\lambda_j^2 \\ B(\xi) &= \lambda_i + \xi^2\lambda_j \end{aligned} \quad .$$

The system Eq. A-2 can be solved, to yield

$$\hat{\omega}_i^2 = \frac{H^2 - \lambda_k^2\hat{\omega}_k^2}{A} \qquad \hat{\omega}_j^2 = \xi^2\hat{\omega}_i^2 \qquad \hat{\omega}_k^2 = \frac{H^2 - 2(A/B)T_{\text{rot}}}{\lambda_k(\lambda_k - A/B)} \quad . \tag{A-3}$$

For a given value of ξ, $\hat{\omega}_k$ may be obtained directly, then $\hat{\omega}_i$ in terms of $\hat{\omega}_k$, and, finally, $\hat{\omega}_j$ in terms of $\hat{\omega}_i$. For the situation at $\psi = \pi/2$ where $\hat{\omega}_i \to 0$ with ξ becoming unbounded, L'Hôpital's Rule can be applied to find value of $\hat{\omega}_j^2$:

$$\hat{\omega}_j^2\Big|_{\psi=\pi/2} = \frac{H^2 - \lambda_k^2\hat{\omega}_k^2}{\lambda_j^2} \quad .$$

As to the term A/B, it monotonically varies from λ_i as $\xi = 0$ to λ_j as $\xi \to \infty$.

So we have solved for the locus of $(\hat{\omega}_1, \hat{\omega}_2, \hat{\omega}_3)$ triplets forming the intersection of the two "conservation" ellipses, in terms of implicit variable ξ. This variable, ξ, is related to the azimuthal angle ψ, located in the i-j plane, by way of Eq. A-1.*

---

*For the degenerate case of axisymmetry, where $\bar{\lambda}_t = \lambda_1 = \lambda_2$, we note several things about the general solution provided in Eq. A-3:

- The term $A/B \to \bar{\lambda}_t$, so that $\hat{\omega}_k \to$ constant,

$$\hat{\omega}_k^2 \to \frac{H^2 - 2\bar{\lambda}_t T_{\text{rot}}}{\lambda_k(\lambda_k - \bar{\lambda}_t)} = \text{const.}$$

- The term $A \to \bar{\lambda}_t(1 + \xi^2) = \bar{\lambda}_t/\cos^2\psi$, so that $\hat{\omega}_i$ becomes a simple cosine function,

$$\hat{\omega}_i^2 = (H^2 - \lambda_k^2\hat{\omega}_k^2)\cos^2\psi \quad .$$

- Because $\xi = \tan\psi$, the term $\hat{\omega}_j$ becomes a simple sine term,

$$\hat{\omega}_j^2 = (H^2 - \lambda_k^2\hat{\omega}_k^2)\sin^2\psi \quad .$$

Since the axisymmetric problem produces a constant value of $\dot{\psi}$, the sinusoidal response of $\hat{\omega}_i$ and $\hat{\omega}_j$ are likewise sinusoidal in time.

A.2 Precessing Axis

As long as the k-axis remains the precessing axis, Eq. A-3 will provide a solution over the complete domain of ψ. However, considering the problem addressed in the main body of this report, if the disruption from axisymmetry is large enough, the k-axis may no longer remain the precessing axis after a mass-ejection event. We can know if this situation has occurred if there exist values of ξ for which no real solution to $\hat{\omega}_k$ exists (this would indicate that that the elliptical intersection is circumnavigating the $\hat{\omega}_i$ or $\hat{\omega}_j$ axis).

Examine more closely the solution for $\hat{\omega}_k^2$ in Eq. A-3. If either the numerator or denominator changes sign with ξ, then one may infer, for some value(s) of ξ, that $\hat{\omega}_k^2 < 0$, implying that no real solution for $\hat{\omega}_k$ exists for that part of the domain. Even when $\hat{\omega}_k = 0$, the condition implies a (momentary) end-over-end tumbling about an axis perpendicular to the k-axis. Either case ($\hat{\omega}_k^2 \leq 0$) means that the k axis is no longer the axis of precession.

Consider first the numerator of $\hat{\omega}_k^2$. Based on the known monotonic variance of A/B between λ_i and λ_j, we may deduce that if $(H^2 - 2\lambda_i T_{\text{rot}})(H^2 - 2\lambda_j T_{\text{rot}})$ is nonpositive, the k-axis is no longer the precessing axis, because it implies that $\hat{\omega}_k$ becomes identically 0 at some point in the i-j azimuth. This exclusionary criterion may be formalized as follows:

$$\text{if } \left(\lambda_i - \frac{H^2}{2T_{\text{rot}}}\right)\left(\lambda_j - \frac{H^2}{2T_{\text{rot}}}\right) \leq 0 \quad \text{, the } k\text{-axis is } \textit{not} \text{ the precessing axis.} \tag{A-4}$$

Given that $\frac{H^2}{2T_{\text{rot}}}$ is bounded by the maximum and minimum principal moments (call them λ_{max} and λ_{min}), we may deduce that the mid-inertial (non-extreme) axis is already precluded from being the precessing axis on the basis that $\lambda_{\text{max}} - \frac{H^2}{2T_{\text{rot}}} \geq 0$ and $\lambda_{\text{min}} - \frac{H^2}{2T_{\text{rot}}} \leq 0$. Thus, their product is always non-positive.

Turn attention to the denominator of $\hat{\omega}_k^2$. If the k-axis is an inertially extreme axis (associated with either λ_{min} or λ_{max}), then $\lambda_k - A/B$ does not change sign as A/B varies from λ_i to λ_j. Therefore, if k is an inertially extreme axis, the term $\lambda_k - A/B$ can in no way play a role in provoking a $\hat{\omega}_k = 0$ solution.

We have already excluded the mid-inertial axis as a possible precessing axis, so we need not consider the effect of the denominator, when k represents the mid-inertial axis. The denominator of $\hat{\omega}_3^2$ thus appears to have no influence on the criterion for determining the precessive axis. And with the mid-inertial axis precluded, there are only two possible axes that can qualify as the precessing axis. If one of them is precluded by way of Eq. A-4, then the other extreme axis *must* be the precessing axis.

Thus, in light of Eq. A-4 and the fact that the denominator of Eq. A-3 plays no role, the precessive axis can be positively determined, regardless of which ijk axis triplet is examined, with the criterion

$$\text{iff } \left(\lambda_i - \frac{H^2}{2T_{\text{rot}}}\right)\left(\lambda_j - \frac{H^2}{2T_{\text{rot}}}\right) > 0 \quad , k \text{ is the precessing axis.} \tag{A-5}$$

A.2.1 Stability of Rotation

The literature tells us[2] that rotation about the mid-inertial axis is unstable, whereas rotation about either of the extreme inertial axes is stable. Does such a result naturally follow from Eq. A-5? The answer is, yes, it does.

For ease of explanation, let us denote and order the three principal moments λ_k as

$$\lambda_{\text{min}} < \lambda_{\text{mid}} < \lambda_{\text{max}} \quad .$$

From Eqs. 43 and 44, one may verify that, in the case of pure rotation about a given principal axis, the value of $\frac{H^2}{2T_{\text{rot}}}$ exactly equals the principal moment of that axis. So, we have the situation that, depending on the components of a given rotation,

$$\lambda_{\text{min}} \le \frac{H^2}{2T_{\text{rot}}} \le \lambda_{\text{max}}$$

and that, when $\frac{H^2}{2T_{\text{rot}}} = \lambda_k$, we have pure rotation about the k-axis.

Consider the two intermediate cases that do not involve pure rotation. First,

$$\lambda_{\text{min}} < \frac{H^2}{2T_{\text{rot}}} < \lambda_{\text{mid}} < \lambda_{\text{max}} \quad .$$

Equation A-5 for this case would indicate that the axis associated with λ_{min} is the

[2] Goldstein H, Poole C, Safko J. Classical mechanics. San Francisco (CA): Addison Wesley; 2002.

precessing axis. This also shows that there is no instability relative to the case where $\frac{H^2}{2T_{\text{rot}}} = \lambda_{\text{min}}$ in which the axis associated with λ_{min} is the spinning axis.

Next,

$$\lambda_{\text{min}} < \lambda_{\text{mid}} < \frac{H^2}{2T_{\text{rot}}} < \lambda_{\text{max}} \quad .$$

Equation A-5 for this case would indicate that the axis associated with λ_{max} is the precessing axis. This also shows that there is no instability relative to the case where $\frac{H^2}{2T_{\text{rot}}} = \lambda_{\text{max}}$ in which the axis associated with λ_{max} is the spinning axis.

On the other hand, the case where $\frac{H^2}{2T_{\text{rot}}} = \lambda_{\text{mid}}$ is immediately seen to be unstable. Why? While the rotation is momentarily about the axis associated with λ_{mid}, an infinitesimal perturbation of $\frac{H^2}{2T_{\text{rot}}}$ will reduce to either one of the two cases discussed previously, with the result that the precessing axis will change over to that associated with either λ_{min} (if the perturbation is negative) or λ_{max} (if the perturbation is positive). There can be no solution for which the mid-inertial axis is the precessing axis.

The discussion, therefore, reduces to an even simpler conclusion:

$$\text{if } \frac{H^2}{2T_{\text{rot}}} \begin{cases} > \lambda_{\text{mid}}, & \text{the precessing axis is that associated with } \lambda_{\text{max}} \\ < \lambda_{\text{mid}}, & \text{the precessing axis is that associated with } \lambda_{\text{min}} \\ = \lambda_{\text{mid}}, & \text{the rotation is unstable} \end{cases} \quad . \qquad \text{(A-6)}$$

This result is presented as Eq. 45 in the main report.

Equation A-6 also explains how the precessing axis of an axisymmetric body will always be the axis of symmetry. If $\lambda_i = \lambda_j$, then Eq. A-6 will always indicate that the k-axis is precessing except when $\frac{H^2}{2T_{\text{rot}}} = \lambda_i = \lambda_j$. And for this lone exception (pure rotation perpendicular to the axis of symmetry), the rotation is unstable, since any small perturbation of $\frac{H^2}{2T_{\text{rot}}}$ will restore k as the precessing axis.

A.3 Application of Analytical Solution (Eq. A-3)

Consider a body with the z-axis (3-axis) as the axis of symmetry. Let the initial value of angular velocity $\hat{\boldsymbol{\omega}} = (0.4,\ 0.4,\ 1)$ be part of the solution space. Such a body will precess with fixed body and space cones. Per Eq. A-5, the 3-axis is necessarily the precessing axis. The body cone, denoting the angle between the precessing axis of symmetry and the angular velocity, given by Eq. 40, will assume a value of $\gamma = 29.5°$ (independent of the moment of inertia).

If, as is the subject of this report, a mass ejection occurs, such that the moment of inertia is no longer axisymmetric, the precession is no longer steady. Let the principal axisymmetric moments of inertia, say $(\lambda_1,\ \lambda_2,\ \lambda_3) = (5,\ 5,\ 1)$, take on a reduced value of λ_1. In Table A-1, the effect of the asymmetry upon the locus of $\hat{\omega}_i$ solutions is presented, for successively lowered values of λ_1, including 4.9, 3, and 2.

Table A-1 Locus of $\hat{\omega}$ as a function of ψ, with $\hat{\omega} = (0.4, 0.4, 1)$ as part of the solution, for (a) $(\lambda_1, \lambda_2, \lambda_3) = (4.9, 5, 1)$, (b) $(\lambda_1, \lambda_2, \lambda_3) = (3, 5, 1)$, and (c) $(\lambda_1, \lambda_2, \lambda_3) = (2, 5, 1)$

ψ (°)	ξ	$\pm\hat{\omega}_1$	$\pm\hat{\omega}_2$	$\pm\hat{\omega}_3$	γ (°)
90.0	∞	0.0000E+00	5.5936E−01	1.0098E+00	28.98
75.0	3.7321E+00	1.4499E−01	5.4110E−01	1.0085E+00	29.05
60.0	1.7321E+00	2.8125E−01	4.8713E−01	1.0049E+00	29.24
45.0	1.0000E+00	4.0000E−01	4.0000E−01	1.0000E+00	29.50
30.0	5.7735E−01	4.9271E−01	2.8447E−01	9.9492E−01	29.76
15.0	2.6795E−01	5.5188E−01	1.4787E−01	9.9111E−01	29.96
0.0	0.0000E+00	5.7223E−01	0.0000E+00	9.8969E−01	30.04

(a)

ψ (°)	ξ	$\pm\hat{\omega}_1$	$\pm\hat{\omega}_2$	$\pm\hat{\omega}_3$	γ (°)
90.0	∞	0.0000E+00	4.5607E−01	1.1136E+00	22.27
75.0	3.7321E+00	1.2091E−01	4.5124E−01	1.1037E+00	22.94
60.0	1.7321E+00	2.5106E−01	4.3485E−01	1.0703E+00	25.13
45.0	1.0000E+00	4.0000E−01	4.0000E−01	1.0000E+00	29.50
30.0	5.7735E−01	5.7308E−01	3.3087E−01	8.6450E−01	37.43
15.0	2.6795E−01	7.4796E−01	2.0042E−01	6.3311E−01	50.73
0.0	0.0000E+00	8.3267E−01	0.0000E+00	4.4721E−01	61.76

(b)

ψ (°)	ξ	$\pm\hat{\omega}_1$	$\pm\hat{\omega}_2$	$\pm\hat{\omega}_3$	γ (°)
90.0	∞	0.0000E+00	4.1952E−01	1.1136E+00	20.64
75.0	3.7321E+00	1.1201E−01	4.1803E−01	1.1051E+00	21.39
60.0	1.7321E+00	2.3827E−01	4.1270E−01	1.0746E+00	23.91
45.0	1.0000E+00	4.0000E−01	4.0000E−01	1.0000E+00	29.50
30.0	5.7735E−01	6.3730E−01	3.6795E−01	7.9421E−01	42.82
18.6	3.3601E−01	9.8654E−01	3.3149E−01	0.0000E+00	90.00

(c)

For the middle case, $\lambda_1 = 3$, the results are graphically portrayed in Fig. A-1. The abscissa ψ, as shown in Fig. A-1, spans 1/4 of the body's azimuthal rotation (quadrant I). The remaining three quadrants of azimuth (II–IV) can be obtained by taking the $(+\hat{\omega}_1, +\hat{\omega}_2)$ solutions, shown above, as $(-\hat{\omega}_1, +\hat{\omega}_2)$, $(-\hat{\omega}_1, -\hat{\omega}_2)$, and $(+\hat{\omega}_1, -\hat{\omega}_2)$, respectively, as provided by the quadratic nature of Eq. A-3.

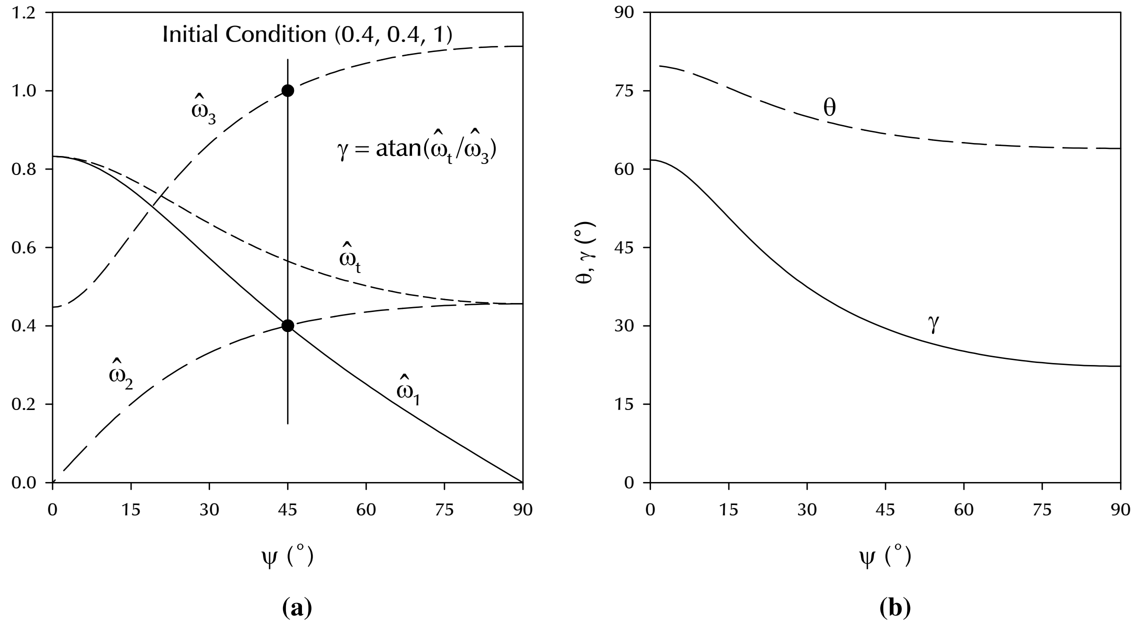

Fig. A-1 Locus of solutions for body with principal moments $(3, 5, 1)$**, subject to initial condition** $\hat{\boldsymbol{\omega}} = (0.4, 0.4, 1)$**: (a)** $\hat{\boldsymbol{\omega}}$**, (b)** ϕ **and** θ

One notes several important features from Table A-1:

- The greater the deviation from axisymmetry, the greater the fluctuation of both the body-cone angle γ as well as the components of $\hat{\boldsymbol{\omega}}$.
- The trend of γ toward 90°, as $\psi \to 0$, in Table A-1b and Fig. A-1b represents a tendency toward a change in the precessive axis.
- If λ_1 gets reduced to a value of 2 (Table A-1c), there are no real solutions for $\hat{\omega}_3$ below $\psi = 18.6°$. Precession has shifted to the 2-axis.
- By applying Eq. A-3 to the 312 triplet* (see Table A-2), rather than the $ijk = 123$ triplet, one may establish that the precession of the case represented in Table A-1c is very stable about the 2-axis, with the body cone angle γ varying only over the range 69.4°–71.4°. The $\hat{\boldsymbol{\omega}} = (0.4,\ 0.4,\ 1)$ solution occurs when $\psi = 21.8°$.

The data in Tables A-1 and A-2 demonstrate an application of Eq. A-3, representing the solution to the intersection of the conservation ellipses (angular momentum

*For the 312 triplet, ψ represents the azimuth in the 3-1 plane and the body-cone angle γ is taken with respect to the 2-axis.

Table A-2 Locus of $\hat{\omega}$ as a function of ψ, with $\hat{\omega} = (0.4, 0.4, 1)$ as part of the solution, with $(\lambda_1, \lambda_2, \lambda_3) = (2, 5, 1)$, but with Eq. A-3 applied to the 312 triplet

ψ (°)	ξ	$\pm\hat{\omega}_3$	$\pm\hat{\omega}_1$	$\pm\hat{\omega}_2$	γ (°)
90.0	∞	0.0000E+00	9.0921E−01	3.0551E−01	71.43
75.0	3.7321E+00	2.3799E−01	8.8820E−01	3.1162E−01	71.28
60.0	1.7321E+00	4.7482E−01	8.2241E−01	3.2919E−01	70.88
45.0	1.0000E+00	7.0427E−01	7.0427E−01	3.5553E−01	70.36
30.0	5.7735E−01	9.0921E−01	5.2493E−01	3.8528E−01	69.85
15.0	2.6795E−01	1.0580E+00	2.8350E−01	4.0983E−01	69.49
0.0	0.0000E+00	1.1136E+00	0.0000E+00	4.1952E−01	69.36

and energy). While the solution gives the locus of $(\hat{\omega}_1, \hat{\omega}_2, \hat{\omega}_3)$ triplets that satisfy the conservation laws, these values do not tell the whole story. In addition to *not* providing time as a variable in the solution, the conservation solution only provides the locus of angular velocities in the principal reference frame. That is to say, the elliptical intersection provides how the angular velocity may proceed with respect to the body coordinates, but not how the body coordinates proceed with respect to the laboratory coordinates. For that, we need to obtain the rates of spin, precession, and nutation.

A.4 Rates of Spin $\dot{\psi}$, Precession $\dot{\phi}$, and Nutation $\dot{\theta}$

When the problem is axisymmetric, the rates of spin and precession may be related back to the angular velocity by way of the body- and space-cone geometries, through Eq. 41 (for axisymmetric torque-free motion, there is no nutation). Even though all the terms are available* for its application, Eq. 41 is no longer valid for non-axisymmetric configurations. However, it is not by chance that the independent variable of the current non-axisymmetric analysis (Eq. A-1) is designated ψ.

When the body is spinning about axis k with an associated precession, the moments in time when $\hat{\omega}_j = 0$ and $\hat{\omega}_i = 0$, respectively, represent body-frame rotational

*Required terms include

$$\hat{\omega} = \sqrt{\hat{\omega}_i^2 + \hat{\omega}_j^2 + \hat{\omega}_k^2}$$

$$\gamma = \tan^{-1}\left(\frac{\sqrt{\hat{\omega}_i^2 + \hat{\omega}_j^2}}{\hat{\omega}_k}\right)$$

$$\theta = \tan^{-1}\left(\frac{\sqrt{\lambda_i^2\hat{\omega}_i^2 + \lambda_j^2\hat{\omega}_j^2}}{\lambda_k\hat{\omega}_k}\right)$$

configurations (ψ) that are $\pi/2$ (90°) apart. According to Eq. A-1, these two configurations are represented as $\psi = 0°$ and $\psi = 90°$, respectively.

The vector $\hat{\boldsymbol{\omega}}$, deriving from the $\hat{\omega}$ components solved in Eq. A-3, may be decomposed into the sum of three vectors: the rates of precession $\dot{\phi}$, spin $\dot{\psi}$, and nutation $\dot{\theta}$. The decomposition, in the principal 1-2-3 reference frame, proceeds as follows:

$$\hat{\boldsymbol{\omega}} = \dot{\phi}\hat{\mathbf{K}} + \dot{\psi}\hat{\mathbf{T}}_k + \dot{\theta}(\hat{\mathbf{T}}_k \times \hat{\mathbf{K}}) \quad . \tag{A-7}$$

In this case, $\hat{\mathbf{K}}$ is the unit vector aligned with the angular momentum (Eq. 31), and $\hat{\mathbf{T}}_k$ is the orientation of the (assumed-precessing) k-axis, *as expressed in the principal coordinate system*. Thus, when considering the $ijk = 123$ triplet, it follows, by definition, that $\hat{\mathbf{T}}_k = \hat{\mathbf{T}}_3 = (0,\, 0,\, 1)$ and, thus, $\hat{\mathbf{K}} \times \hat{\mathbf{T}}_3 = (-\hat{K}_2,\, \hat{K}_1,\, 0)$.

For the case where the 3-axis precesses, the system Fig. A-7 reduces to the following set of equations:

$$\begin{aligned}
\hat{\omega}_1 &= \hat{K}_1\dot{\phi} - \hat{K}_2\dot{\theta} \\
\hat{\omega}_2 &= \hat{K}_2\dot{\phi} + \hat{K}_1\dot{\theta} \quad . \\
\hat{\omega}_3 &= \hat{K}_3\dot{\phi} + \dot{\psi}
\end{aligned}$$

This system may be solved as

$$\begin{aligned}
\dot{\phi} &= \frac{\hat{K}_1\hat{\omega}_1 + \hat{K}_2\hat{\omega}_2}{\hat{K}_1^2 + \hat{K}_2^2} &&= \frac{\hat{K}_1\hat{\omega}_1 + \hat{K}_2\hat{\omega}_2}{\sin^2\theta} \\
\dot{\theta} &= \frac{\hat{K}_1\hat{\omega}_2 - \hat{K}_2\hat{\omega}_1}{\hat{K}_1^2 + \hat{K}_2^2} &&= \frac{\hat{K}_1\hat{\omega}_2 - \hat{K}_2\hat{\omega}_1}{\sin^2\theta} \quad . \\
\dot{\psi} &= \hat{\omega}_3 - \hat{K}_3\dot{\phi} &&= \hat{\omega}_3 - \dot{\phi}\cos\theta
\end{aligned} \tag{A-8}$$

Equation A-8 provides the key variables of the precessing body in terms of the $\hat{\boldsymbol{\omega}}$ components, which themselves are expressed in terms of ψ by way of Eqs. A-1 and A-3.

For cases where the body geometry is axisymmetric, $\hat{\boldsymbol{\omega}}$ is coplanar with $\hat{\mathbf{H}}$ and $\hat{\mathbf{T}}_k$, with the result being that $\dot{\theta} \equiv 0$. In such cases, the result of Eq. A-8 matches that of Eq. 41 (a constant $\dot{\psi}$ and $\dot{\phi}$, independent of ψ). But where geometry diverges from axisymmetry, the results differ because the (coplanar) premise used to derive Eq. 41 is no longer valid. One may take Eq. A-8 and apply it to, for example, the case described in Fig. A-1 to obtain the result presented in Fig. A-2. Note that in azimuthal quadrants II and IV, the nutation rate $\dot{\theta}$ will be positive.

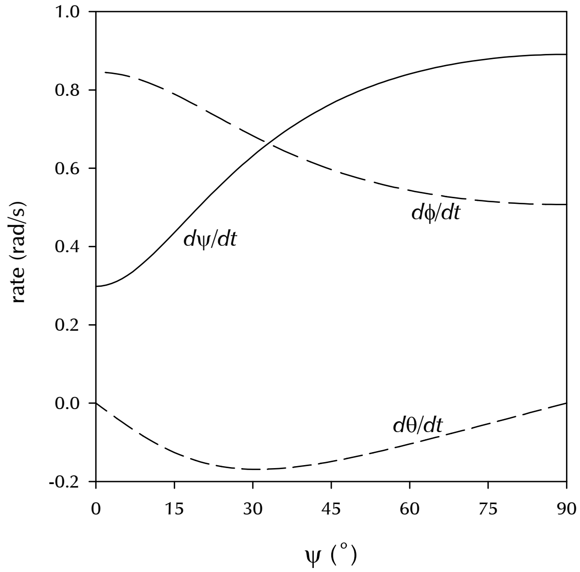

Fig. A-2 Locus of solutions for body spin rate $\dot{\psi}$, precession rate $\dot{\phi}$, and nutation rate $\dot{\theta}$ with principal moments $(3, 5, 1)$, subject to initial condition $\hat{\omega} = (0.4, 0.4, 1)$

A.5 Completing the Solution

Because this approach arises out of the algebraic solution to the intersection of two ellipses, the one thing missing from the solution embodied in Eqs. A-1, A-3, and A-8 is the element of time. There is not a closed-form solution in this case, but the element of time is quite easily recovered. For a given set of initial conditions, we can literally tabulate (in the manner of Table A-1) $\dot{\psi}$ in terms of ψ using any suitably small increment $\Delta\psi$. The time required to transition from a specific ψ_x to the adjacent ψ_{x+1} is approximated by the difference equation $\Delta t_{x+\frac{1}{2}} \approx 2\Delta\psi/(\dot{\psi}_x + \dot{\psi}_{x+1})$.

Over the same spin increment $\Delta\psi$, the increment of precession may likewise be recovered as $\Delta\phi_{x+\frac{1}{2}} \approx \Delta\psi(\dot{\phi}_x + \dot{\phi}_{x+1})/(\dot{\psi}_x + \dot{\psi}_{x+1})$ (note that $\dot{\theta}$ need not be integrated, as θ is already available directly, given $\hat{\omega}_i$ and λ_i, by way of Eq. 39). These increments of Δt and $\Delta\phi$ may be summed to achieve t and ϕ as a function of our independent variable ψ:

$$t_n - t_k = \sum_{i=k}^{n-1} \Delta t_{i+\frac{1}{2}} \qquad\qquad \phi_n - \phi_k = \sum_{i=k}^{n-1} \Delta\phi_{i+\frac{1}{2}}$$

If t, ϕ, and θ are all known as a function of ψ, they may be used in conjunction with the angular momentum vector in the laboratory frame, $\mathbf{H}'_{G'}$, to characterize the motion of the body in the laboratory frame of reference.

Using a tabulation with a $\Delta\psi = 1°$, the integration was performed on the problem of Table A-1b (see also Fig. A-1). The results, providing the integrated t and ϕ functions, are presented in 15° increments in Table A-3. The associated data are graphically shown in Fig. A-3. Were the precession regular, $\psi(t)$ and $\phi(t)$ would be linear and θ and γ would be constant. As it is, the nutation θ is nearly sinusoidal in time. The spin ψ requires significantly more time over the range $0 \leq \psi < 45°$ than it does over the range $45° \leq \psi \leq 90°$.

Table A-3 Precession variables for body with principal moments $(3, 5, 1)$, subject to initial condition $\hat{\boldsymbol{\omega}} = (0.4, 0.4, 1)$

ψ	t **(s)**	γ **(°)**	θ **(°)**	ϕ **(°)**	$\dot{\psi}$ **(rad/s)**	$\dot{\phi}$ **(rad/s)**	$\dot{\theta}$ **(rad/s)**
90	0.9234	22.27	63.97	28.40	0.8908	0.5075	0.0000
75	0.6283	22.94	64.22	19.76	0.8792	0.5161	−0.0530
60	0.3248	23.13	65.06	10.58	0.8409	0.5438	−0.1047
45	0.0000	29.50	66.79	0.00	0.7647	0.5971	−0.1493
30	−0.3731	37.43	70.08	−13.66	0.6318	0.6832	−0.1691
15	−0.8656	50.73	75.55	−34.53	0.4361	0.7896	−0.1260
0	−1.6249	61.76	79.85	−70.56	0.2981	0.8459	0.0000

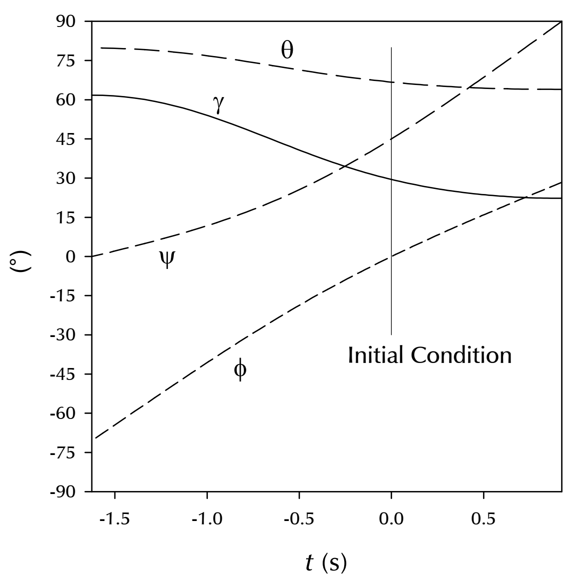

Fig. A-3 Precession variables presented as a function of time, for body with principal moments $(3, 5, 1)$, subject to initial condition $\hat{\boldsymbol{\omega}} = (0.4, 0.4, 1)$

1 (PDF) DEFENSE TECHNICAL
INFORMATION CTR
DTIC OCA

2 (PDF) DIR ARL
IMAL HRA
RECORDS MGMT
RDRL DCL
TECH LIB

1 (PDF) GOVT PRINTG OFC
A MALHOTRA

1 (PDF) COMMANDER
US ARMY ARDEC
R FONG

1 (PDF) COMMANDER
US ARMY AVN & MISSILE CMD
S CORNELIUS

1 (PDF) NSWC
INDIAN HEAD DIVISION
T P MCGRATH II

1 (PDF) NAVAIR
E SIEVEKA

1 (PDF) NATICK SOLDIER RD&E CENTER
M E ROYLANCE

1 (PDF) US ARMY ERDEC
J Q EHRGOTT JR

1 (PDF) ATR CORP
A WARDLAW

1 (PDF) SOUTHWEST RESEARCH INST
T HOLMQUIST

3 (PDF) DE TECHNOLOGIES
R CICCARELLI
W FLIS
W CLARK

1 (PDF) IDEAL INNOVATIONS INC
D E SIMON

1 (PDF) APPLIED RESEARCH ASSOC INC
R T BOCCHIERI

1 (PDF) DREXEL UNIVERSITY
B FAROUK

ABERDEEN PROVING GROUND

105 (PDF) DIR USARL
RDRL DP
T ROSENBERGER
RDRL SL
P BAKER
RDRL SLB
R BOWEN
RDRL SLB A
D FORDYCE
RDRL SLB D
R GROTE
L MOSS
J POLESNE
RDRL SLB E
M MAHAFFEY
C BARKER
R CIAPPI
C COWARD
D HOWLE
RDRL SLB G
P MERGLER
J ABELL
P HORTON
RDRL SLB S
M PERRY
D LYNCH
J SHINDELL
RDRL SLB W
R BOWERS
W MERMAGEN
RDRL WM S SCHOENFELD
RDRL WML A
W OBERLE
B BREECH
RDRL WML C
K MCNESBY
B ROOS
RDRL WML E
P WEINACHT
RDRL WML F
J CONDON
RDRL WML H
T EHLERS
E KENNEDY
L MAGNESS
C MEYER
B SORENSEN
R SUMMERS
RDRL WMM B
B LOVE
G GAZONAS

RDRL WMM C
R JENSEN
RDRL WMM D
S WALSH
RDRL WMM E
P PATEL
RDRL WMP
D LYON
J HOGGE
T VONG
RDRL WMP A
S R BILYK
P BERNING
J CAZAMIAS
M COPPINGER
J FLENIKEN
W C UHLIG
C WOLFE
RDRL WMP B
C HOPPEL
M J GRAHAM
S SATAPATHY
RDRL WMP C
M FERMEN-COKER
R BECKER
T BJERKE
D CASEM
J CLAYTON
M GREENFIELD
B LEAVY
J LLOYD
S SEGLETES
L SHANAHAN
A SOKOLOW
A TONGE
W WALTERS
C WILLIAMS
RDRL WMP D
J RUNYEON
A BARD
N BRUCHEY
R DONEY
S HALSEY
M KEELE
D KLEPONIS
H W MEYER
R MUDD
F MURPHY
D PETTY
C RANDOW
S SCHRAML
B SCOTT
K STOFFEL
G VUNNI
V WAGONER
M ZELLNER
RDRL WMP E
P SWOBODA
P BARTKOWSKI
D GALLARDY
D HACKBARTH
D HORNBAKER
E HORWATH
J HOUSKAMP
E KLIER
C KRAUTHAUSER
M LOVE
K MCNAB
D SHOWALTER
RDRL WMP F
N GNIAZDOWSKI
C CUMMINS
E FIORAVANTE
D FOX
R GUPTA
S HUG
RDRL WMP G
R FRANCART
S KUKUCK
C PECORA
J STEWART